Journal of Shellfish Research, Vol. 44, No. 3, 547–562, 2025.

DIFFERENCES IN DIGESTIVE ENZYME ACTIVITIES, MICROBIAL DIVERSITY, AND GASTROINTESTINAL FERMENTATION IN RED ABALONE (*HALIOTIS RUFESCENS*) AND PĀUA (*HALIOTIS IRIS*)

A. M. LEE,[1] L. ASHLOCK,[2] M. J. HERRERA,[1,3] D. P. GERMAN[1] AND A. R. FREDERICK[2]*

[1]*Department of Ecology and Evolutionary Biology, 321 Steinhaus Hall, University of California, Irvine, CA 92617;* [2]*Bodega Marine Laboratory, University of California, Davis, P.O. Box 247, 2099 Westshore Rd, Bodega Bay, CA 94923;* [3]*Marine Biology Research Division, Scripps Institution of Oceanography, 8622 Kennel Way, University of California, San Diego, CA 92093*

ABSTRACT Abalone are large, marine, herbivorous gastropods that hold great cultural, ecological, and economic importance across the world. Many abalone species are cultured for food or conservation, and there is a dense literature on their feeding habits and digestive physiology in captive settings. There has been, however, little investigation of the digestive physiology or enteric microbial diversity of wild-caught abalone. Thus, an examination of the microbial diversity and levels of gastrointestinal fermentation was performed in different regions of the gut of wild-caught red abalone (*Haliotis rufescens*) from the northeastern Pacific (California), and in pāua (*Haliotis iris*) from the southwestern Pacific (Aotearoa New Zealand). Digestive enzyme activities were also measured in the digestive gland/stomach of the two species. It was observed that, similar to other abalone, these two abalone species harbored a similar microbiome all the way to the genus level, with *Mycoplasma* (Phylum Mycoplasmatota), *Vibrio* (Phylum Pseudomonodota), and *Psychrilyobacter* (Phylum Fusobacteriota) composing the majority of sequence reads. There was variation in indicator species among gut regions, and between gut tissue and luminal contents of each region, showing that there is variation axially and radially in the gut. Concentrations of short-chain fatty acids were similar among gut regions in each species, but *H. rufescens* tended to have more butyrate in their guts than *H. iris*. Digestive enzyme activities were similar among the two abalone species, but *H. iris* had two orders of magnitude higher acid phosphatase activities. Overall, this is one of the most detailed analyses of wild-caught abalone digestive physiology and sets a baseline for comparison with animals being reared in captivity.

KEY WORDS: digestion, mollusc, aquaculture, microbiome, herbivory

INTRODUCTION

Abalone are large, marine gastropods that hold immense economic, cultural, and ecological value globally (Leighton 2000, Vileisis 2020). In fact, given their size and the beauty of their shells, abalone are harvested from the wild or farmed for conservation and/or human consumption throughout the world (Bullon et al. 2023). As herbivores, abalone are considered an important aspect of sustainable aquaculture (Naylor et al. 2021, Bullon et al. 2023). Thus, there is a dense literature on abalone dietary habits and digestion in captive settings (Tahil & Juinio-Menez 1999, Garcia-Esquivel & Felbeck 2006, Cornwall et al. 2009, Zeeman et al. 2012, Stone et al. 2013, Bansemer et al. 2016, Ansary et al. 2019). From these studies, researchers have learned about the common microbes that inhabit their guts (Guo 2017, Gobet et al. 2018, Nam et al. 2018, Parker-Graham et al. 2020, Cicala et al. 2023, Hur et al. 2023, Liu et al. 2023), the algae or formulated diets that the abalone tend to thrive on, and how to grow the animals quickly (Bullon et al. 2023). There is, however, a paucity of studies on digestion in wild-caught abalone, gauging the activity levels of digestive enzymes, how microbial communities vary in different gut regions, and the levels of gastrointestinal fermentation in the form of short-chain fatty acid (SCFA) concentrations within the abalone digestive system. For some time, it has been clear that there are microbes capable of fiber digestion (Erasmus et al. 1997) and gastrointestinal fermentation in abalone guts (Sawabe et al. 2003, Tanaka et al. 2003), yet there are few studies that have actually measured SCFA concentrations in abalone alimentary canals (Iehata et al. 2009, Iehata et al. 2010) to examine how different gut regions might vary in terms of microbial function.

Digestion is a chemical process catalyzed by digestive enzymes. These enzymes can come from the host or from microbes inhabiting animal guts. Unlike vertebrates, abalone have the genes to synthesize digestive enzymes that can degrade plant fibers (e.g., cellulose, alginate; Gómez-Pinchetti & García-Reina 1993, Li et al. 2023), as well as the more soluble portions of algae (Picos-García et al. 2000, Garcia-Esquivel & Felbeck 2006, Li et al. 2023, Wang et al. 2024). As with understanding how microbial communities vary along the gut, few studies have examined how digestive enzyme activities vary along the abalone digestive system (Picos-García et al. 2000, Garcia-Esquivel & Felbeck 2006, Nel et al. 2017), with many enzymatic activities being highest in the stomach/digestive gland (Garcia-Esquivel & Felbeck 2006, Frederick et al. 2022). Given that digestive enzyme activities correlate with digestibility (Karasov & Douglas 2013), measuring enzymatic activities provides insight into how well abalone can digest aspects of their algal diet.

Apart from the few abalone species that are cultured for food (e.g., *Haliotis discus hannai, Haliotis tuberculata*), most wild abalone remain poorly studied in terms of their digestive physiology. This is true whether one is interested in the north or south Pacific. Thus, in this study, the enteric microbial communities, and concentrations of SCFAs (microbial byproducts of fermentation) were examined along the digestive systems of abalone from opposite ends of the Pacific Ocean: red abalone (*Haliotis rufescens*) in the eastern north Pacific, and pāua (*Haliotis iris*) from the western south Pacific. Because the

*Corresponding author. E-mail: abrac@ucdavis.edu
DOI: 10.2983/035.044.0319

stomach/digestive gland produces a broad array of digestive enzymes, enzymatic activity measurements were performed in this gut region of the two species.

Although there are some phylogenies available for abalone (Estes et al. 2005, Masonbrink et al. 2019), a phylogeny was generated for the abalone of the northeastern Pacific, using *Haliotis iris* as an outgroup (Frederick 2019; see Appendix for detailed phylogenetic methods). *Haliotis rufescens* are the largest abalone species in the world, reaching as large as 31 cm in shell length (Leighton 2000), and they are part of a cold-water clade that includes the endangered white abalone (*Haliotis sorenseni*), the pinto abalone (*Haliotis kamtschatkana*), and the flat abalone (*Haliotis walallensis*; Fig. 1). Pāua (*H. iris*) hold similar value in Aotearoa New Zealand, and are distantly related to this northeastern Pacific clade of abalone (Fig. 1, Estes et al. 2005). The range for *H. rufescens* spans from southern Oregon, United States, to Baja California, Mexico, with a depth range from the intertidal (in their northern range only) to 24 m (California Department of Fish and Wildlife 2005). Pāua live in the rocky shore habitat around most of Aotearoa New Zealand, including the Chatham Islands, preferring shallower habitat to 12 m depth with a preference for around 5–6 m under boulders (Schiel & Breen 1991, Schiel et al. 1995). Both species graze on macroalgae present in their environments. Pāua generally prefers feeding on drift algae, primarily the kelp *Lessonia variegata*, but will also feed on red and green algae (Cornwall et al. 2009).

To examine the function of the digestive systems of *Haliotis rufescens* and *Haliotis iris*, the digestive systems were divided into the mouth, esophagus, digestive gland, which sits atop the stomach, the stomach itself (Harris et al. 1998), and the intestine, divided into proximal and distal regions (Frederick et al. 2022). Given that many studies on abalone digestion treat the gut as a single organ (Bansemer et al. 2016, Li et al. 2023), this is one of the most detailed studies of microbiomes and SCFA concentrations in any abalone species to date, simply by taking the gut region into account. Gut function varies depending on region because the digestive system is compartmentalized (Penry & Jumars 1987, Penry 1989, Horn & Messer 1992, Harris et al. 1998, Garcia-Esquivel & Felbeck 2006, Nel et al. 2017, Lyu et al. 2023). Thus, the following hypotheses were generated regarding the microbiomes of the abalone: (1) The highest microbial diversity would be in the stomach, because the pH of this organ more resembles that of a rumen (Van Soest 1994, Harris et al. 1998) than it does the gastric stomach seen in vertebrates (Wilson & Castro 2010); (2) Because of the pH of the stomach (pH 5–6; Harris et al. 1998, Frederick et al. 2022), the concentrations of SCFA would be highest in this gut region in comparison with the intestine, which is more of a simple tube in abalone; and (3) Because *H. rufescens* and *H. iris* inhabit different ocean basins, consume different algal taxa, and are not closely related (Fig. 1), their microbiomes should be strongly different. Because many abalone taxa share many of the same bacterial phyla in their guts (Guo 2017, Gobet et al. 2018, Nam et al. 2018, Parker-Graham et al. 2020, Cicala et al. 2023, Hur et al. 2023, Liu et al. 2023), the same is expected here, but the separation of the species by 10,800 km, should mean that the microbial species will vary among *H. rufescens* and *H. iris*.

In terms of digestive enzyme activities, expectations were based on the adaptive modulation hypothesis, which states that gut function (especially digestive enzyme activities and nutrient transporters) should match with ingested dietary nutrient concentrations, because, otherwise, enzyme synthesis would be wasted on low-concentration substrates for those enzymes (Karasov 1992, Karasov & Martínez del Rio 2007, Karasov et al. 2025). The activities of carbohydrases (amylase, maltase, β-glucosidase), proteases (trypsin, alanine aminopeptidase, leucine aminopeptidase), and a phosphate acquiring enzyme (acid phosphatase) were measured. There is excellent support for the adaptive modulation hypothesis for carbohydrases, as animals that ingest more starch tend to have elevated amylolytic activities in comparison with animals that do not ingest as much starch (Perry et al. 2007, Axelsson et al. 2013, German et al. 2016). In this case, with both abalone species consuming algal diets dominated by brown and red algae, one would predict elevated carbohydrase activities (amylase in particular) in their digestive glands, and lower proteolytic activities, and not much differences among the species. Previous measurements found that *H. iris* does not express a working alanine aminopeptidase enzyme in its digestive gland (Frederick et al. 2022), so similar results were expected here with detectable alanine aminopeptidase in *H. rufescens*, but not *H. iris*.

Given that nutrient acquisition is central to the survival of an animal, examining digestion is key to understand how animals make a living. Moreover, the dearth of information on digestion in wild-caught abalone means there is no baseline for what the enteric microbiome, SCFA concentrations, and digestive enzyme activities look like in wild animals versus farmed ones. Thus, to better understand digestion in farmed abalone, comparisons with the wild condition are necessary, which this study begins to do for *Haliotis rufescens* and *Haliotis iris*, each of which are farmed in California and to a lesser degree in Aotearoa New Zealand, respectively.

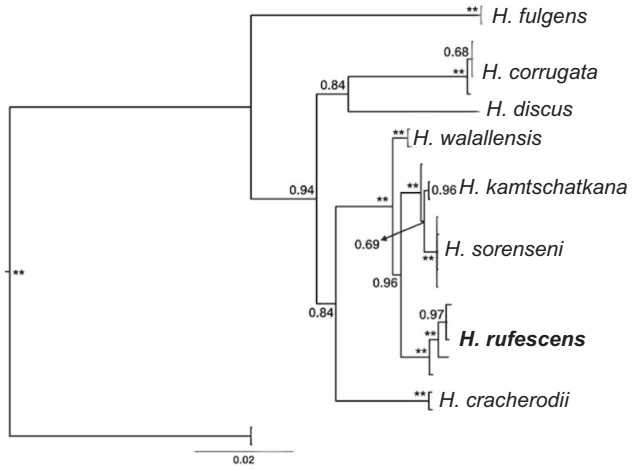

Figure 1. Bayesian phylogenetic tree for the *Haliotis* species on the west coast of North America, using *H. iris* as an outgroup. The tree is based on sequences of 16S, cyt *b*, H3, and ITS1 genes. The percentage of times that a particular node was recovered in 10 million generations of Markov Chain Monte Carlo is listed as the Bayesian posterior probability, with ** signifying $P \geq 0.99$. Pāua (*H. iris*) and red abalone (*H. rufescens*) are bolded. See Appendix for methodology and specimen details.

MATERIALS AND METHODS

Animal Collection and Dissections

Red abalone (*Haliotis rufescens*) (n = 12) were collected on October 29, 2017 by recreational fishers at Van Damme State Park (123° 47′ 30.2″ W, 39° 16′ 23.3″ N). A special salvage permit was issued, allowing for field sampling of legally harvested recreational abalone take under Scientific Collecting Permit #13783 from the California Department of Fish and Wildlife, to PI Alyssa Frederick. A total of N = 3 males and N = 9 females were collected. The average (±standard deviation) length was 197 ± 10 mm, and the average mass of the animals was 1548 ± 257 g.

Pāua (*Haliotis iris*) (n = 4) were collected on April 19, 2018 from Kau Bay, Wellington, New Zealand (41° 17′ 17.5″ S 174° 49′ 47.4″ E). Additional pāua (n = 8) were collected on May 7, 2018 from both Breaker Bay and Princess Beach, Houghton Bay on the southern coast of Wellington, New Zealand. All collections were performed by divers at the Victoria University of Wellington Coastal Ecology Laboratory. The animals were dissected within hours of collection. The average (±standard deviation) length was 125 ± 8 mm, and the average mass of the animals was 260 ± 71 g.

Following the methods of Frederick et al. (2022), animals were placed on crushed ice as an anesthetic until unresponsive. Animals were measured for total wet mass, shell mass (after removing the soft tissue), and the longest length of the shell. Each animal was removed from its shell by severing the foot muscle attachment to the shell. The head was severed from the rest of the body swiftly to ensure the animals were deceased before dissections. Dissections were performed on a metal tray thoroughly cleaned with 70% ethanol, which was filled with ice to keep the dissection surface cold. Instruments and surfaces were thoroughly cleaned with ethanol between tissue types and specimens (Herrera et al. 2025). As in Frederick (2019), the entire digestive system was separated by region: radula (mouth), esophagus, digestive gland, stomach, proximal intestine, and distal intestine. Gut contents (digesta) were separated from gut tissue for each gut region using ethanol-cleaned forceps and the blunt side of a razor blade. For each gut region, the tissues and contents were placed in separate 15 mL centrifuge vials (that had been exposed to UV radiation before use) and immediately flash-frozen. All *Haliotis rufescens* samples were frozen and transported in liquid nitrogen, and *Haliotis iris* samples were frozen in a -80°C freezer and transported on dry ice to University of California, Irvine. They were stored at -80°C until processed.

Digestive Enzyme Assays

Frozen digestive glands samples were weighed and homogenized before thawing in ice-cold citric acid sodium citrate buffer at a pH of 5.6 (the pH measured in the digestive gland of *Haliotis rufescens* using pH paper by Frederick et al. 2022) using a Polytron homogenizer (Brinkman Instruments; Westbury, NY) in 30-sec pulses. Connective tissue was removed. Homogenized samples were centrifuged at 9,400 × g for 2 min at 4°C, then the supernatant was stored in 100–130 µL aliquots at -80°C until used in assays (German et al. 2015). The biochemical activity levels of three carbohydrases (amylase, maltase, and β-glucosidase), three proteases (trypsin, alanine-aminopeptidase, and leucine-aminopeptidase), and acid phosphatase were measured using digestive gland homogenate supernatants, following the methods of Frederick et al. (2022) and German et al. (2004). Assays for carbohydrases, alanine-aminopeptidase, leucine-aminopeptidase, and acid phosphatase were run at pH 5.6, which was the average pH measured in the digestive glands of dissected abalone using pH paper (Frederick et al. 2022). Trypsin was measured at pH 7 because the substrate precipitated out of solution at a lower pH. The temperatures used for the assay incubations matched those of the collection site around the time of collection and dissection (12°C for *Haliotis rufescens* and 14°C for *Haliotis iris*). On its face, this should lead to an expectation of higher enzymatic activities in *H. iris* just due to temperature differences used in the assays. Yet, when these same abalone species were reared at a lower temperature and an elevated temperature that was 5°C higher than the lower temperature, little temperature sensitivity of the digestive enzyme activities was detected (Frederick et al. 2022). Moreover, the comparison among the species here is limited and extreme differences are the focus, as subtle ones can have too many potential explanatory variables with a two-species comparison.

Microbiome Analyses

The sample DNA was isolated from the tissue of the radula (mouth), esophagus, stomach, digestive gland lumen (just called digestive gland), stomach, proximal intestine, and distal intestine, as well as from the contents of the digestive gland, stomach, proximal intestine, and distal intestine using the Zymobiomics DNA mini kit from Zymo Research. Amplicon polymerase chain reaction (PCR) of 16S rDNA was performed targeting the V4–V5 region using the Earth Microbiome Project primers (Caporaso et al. 2012, Walters et al. 2016). The libraries were sequenced at the University of California, Irvine Genomics Research and Technology Hub (GRTH) using a miseq v3 chemistry with a PE300 sequencing length. Sequencing resulted in 18.7 M reads passing the filter. An additional miseq run was conducted with additional samples that had low-quality scores, and the amplicon sequence variants data were merged in QIIME2 (version 2020.8). The raw sequences were imported into QIIME2 using the UCI High Performance Community Computing Cluster (HPC3). After initial sample quality check (99% identity threshold), the paired-end sequences were quality filtered using the DADA2 pipeline in QIIME2, resulting in 2.8 million merged paired-end reads. The first 5 bp were then trimmed, and the forward read was truncated at 285 bp with the reverse read truncated at 248 bp. Taxonomic classification for amplicon sequence variants was assigned using the Silva 138 99% OTUs from the 515F/926R region of sequences (Quast et al. 2012). Analyses were conducted in QIIME2, and the feature table was imported into R (Version 1.4.1103). Within R, we used Shannon alpha diversity and One-way ANOVA followed by Tukey HSD to determine what gut regions were different in alpha diversity within each species. Alpha diversity was not statistically compared between the two species. A Bray–Curtis Dissimilarity matrix was used to examine beta diversity and to construct a nonmetric multidimensional scaling plot. To test for differences among samples, a PERMANOVA with 999

permutations was used, as well as a pairwise PERMANOVA using Benjamini–Hochberg *P*-adjusted values. To determine which microbial taxa were driving differences in gut regions or among the two abalone species, indicator species analysis was run with each gut region in a species as different "habitats" (De Cáceres et al. 2012). This analysis shares what taxa are uniquely abundant in a given sample type (species or gut region).

Measurement of Short Chain Fatty Acids

Measurements of symbiotic fermentation activity were based on the methods of Pryor and Bjorndal (2005), as described in Leigh et al. (2021). Fermentation activity was indicated by relative concentrations of SCFA in the fluid of the stomach, proximal intestine, and distal intestine of *Haliotis rufescens* and *Haliotis iris*. Stomach and intestinal contents were frozen, individually, in sterile centrifuge vials. Gut content samples were weighed, thawed, homogenized with a vortex mixer, and centrifuged under refrigeration (4°C) at 16,000 × g for 10 min. The supernatant was then pipetted into a sterile centrifuge vial equipped with a 0.22 µm cellulose acetate filter (Costar Spin-X gamma sterilized centrifuge tube filters; Coming, NY) and centrifuged under refrigeration at 13,000 × g for 5 min to remove particles from the fluid (including bacterial cells). The filtrates were collected and frozen until they were analyzed for SCFA concentrations.

Concentrations of SCFA in the gut fluid samples from the stomach, intestine, and distal intestine were measured using gas chromatography. Fluid filtrates were hand-injected into an Agilent Technologies 7890A gas chromatograph equipped with a flame ionization detector. Two microliters of each filtrate were injected onto a 2-m-long stainless steel column (3.2 mm ID) packed with 10% SP-1000 and 1% H_3PO_4 on 100/120 Chromosorb W AW (Supelco Inc., Bellefonte, PA). An external standard containing 100 mg L^{-1} each of acetate, propionate, isobutyrate, butyrate, isovalerate, and valerate was used for calibration. A 20% phosphoric acid solution was used to clear the column between samples, followed by rinses with nanopure water. The SCFA concentrations are expressed as mM L^{-1} of gut fluid (volumetric concentration) and are not based on the amount of fluid recovered from any one gut region.

Statistical Analysis

Statistics were run in R Studio version 4.1.1 (R Core Team 2020). Enzyme activities were compared among the species for each enzyme individually using one-way ANOVA. For the SCFA analyses, one-way ANOVA tests were used for intraspecific comparison of individual SCFA (acetate, propionate, and butyrate) concentrations among the gut regions. Interspecific comparisons of each SCFA (and total SCFA) for each gut region (e.g., stomach versus stomach) were made with *t*-tests with a Bonferroni Correction for multiple comparisons. Prior to parametric tests, the Bartlett test for homoscedasticity and the Shapiro–Wilk test for normality were performed on all enzyme datasets (Levene's test for the SCFA data). Where necessary to normalize the data, log, square-root, or exponential (Box-Cox) transformations were used (Table 1).

RESULTS

Digestive Enzyme Activities and Short Chain Fatty Acid Concentrations

Acid phosphatase activity in *Haliotis iris* was over two orders of magnitude higher than that in *Haliotis rufescens* (Table 1; Fig. 2; $P < 0.001$). Trypsin activity did not differ significantly between the two species ($P = 0.117$). Leucine-aminopeptidase activity was 146% higher in *H. iris* relative to *H. rufescens* (Table 1; Fig. 2; $P < 0.001$). Alanine-aminopeptidase was only detectable in *H.* rufescens, and the average (±standard deviation) activity level was 14.40 ± 10.09 µmol min^{-1} g^{-1} (Fig. 2). Amylase activity in *H. iris* was over twice that found in *H. rufescens* (Fig. 2, Table 1, $P = 0.002$). Maltase activity was 68% higher in *H. iris* than in *H. rufescens* (Fig. 2, Table 1, $P = 0.005$). β-glucosidase activity did not differ significantly between the two species ($P = 0.497$).

In terms of the SCFAs, *Haliotis iris* showed significant differences in acetate concentration by gut region, with the stomach having significantly lower acetate than the proximal intestine or distal intestine, which in turn did not differ from one another ($F_{2,30 = 9.018}$; $P < 0.001$; Fig. 3). Propionate ($F_{2,30 = 1.182}$; $P = 0.321$) and butyrate ($F_{2,30 = 0.177}$; $P = 0.838$) concentrations did not vary among the gut regions in *H. iris* (Fig. 3). In *Haliotis rufescens*, there were no differences among the gut regions for acetate ($F_{2,33 = 0.029}$; $P = 0.972$), propionate ($F_{2,33 = 1.515}$; $P = 0.2188$), or

TABLE 1.

Summary statistics for all enzyme activity data in the digestive glands of *H. rufescens* and *H. iris*.

	Sample size (*n*)		Mean ± SD		ANOVA			
Metric	*H. rufescens*	*H. iris*	*H. rufescens*	*H. iris*	*F*	df	*P*	Transformation
Acid phosphatase activity (nmol min^{-1} g^{-1})	11	11	60.41 ± 31.90	7390 ± 4349	334.4	1,20	**5.92E-14*** **	log
Trypsin activity (µmol min^{-1} g^{-1})	10	12	0.36 ± 0.28	0.57 ± 0.32	2.69	1,20	0.117	NA
Leucine-aminopeptidase activity (nmol min^{-1} g^{-1})	12	12	37.42 ± 19.17	91.88 ± 55.14	14.6	1,22	**9.32E-04*** **	sqrt
Amylase activity (µmol min^{-1} g^{-1})	12	12	1.25 ± 0.62	3.93 ± 2.94	12.87	1,22	**1.64E-03** **	$x^{0.25}$
Maltase activity (µmol min^{-1} g^{-1})	12	12	1.37 ± 0.70	2.30 ± 0.73	10.02	1,22	**4.48E-03** **	NA
β-Glucosidase activity (nmol min^{-1} g^{-1})	11	11	16.34 ± 11.55	13.30 ± 12.04	0.479	1,20	0.497	sqrt

Sample sizes indicate the number of analyzed samples in each species and assay. Mean ± SD within each heat treatment is shown, with *F*-statistic and degrees of freedom (treatment, residuals) for every ANOVA. For significant differences among the species for a given enzyme, the *P* values are bolded and ** indicates $P < 0.01$ and *** indicates $P < 0.001$. When data were transformed to better meet the assumptions of normality and homoscedasticity, the transformation used on the raw data is also indicated. "NA" signifies that no transformation was used.

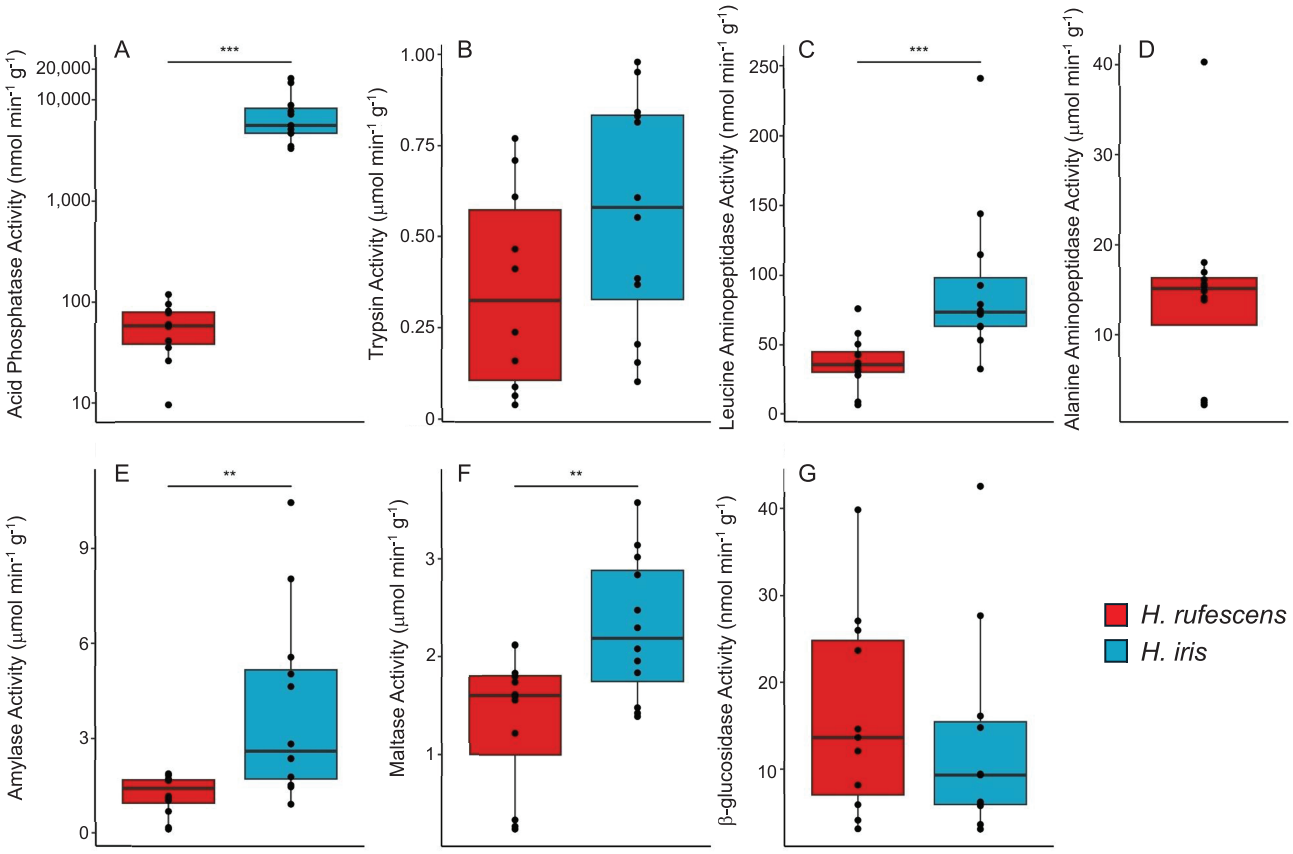

Figure 2. Box plots of digestive enzyme activities in the digestive glands of *Haliotis rufescens* (from California) and *Haliotis iris* (from New Zealand). For each enzyme, data were compared among the species with ANOVA or a sufficient nonparametric test. Differences are indicated with asterisks ($P < 0.01$; *** $P < 0.001$). Comparisons with no asterisk were not statistically different ($P > 0.05$). Note that *H. iris* lacks alanine-aminopeptidase activity.**

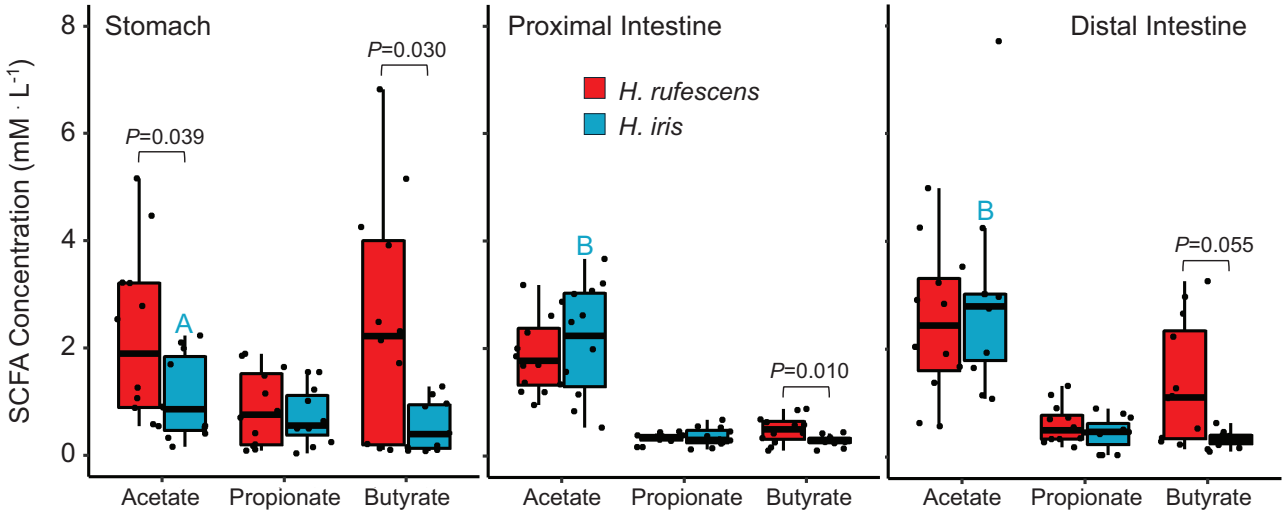

Figure 3. Volumetric concentrations of the short-chain fatty acids (SCFA) acetate, propionate, and butyrate in different gut regions of *Haliotis rufescens* and *Haliotis iris* captured from the wild. Intraspecific comparisons of each SCFA were made among gut regions with ANOVA followed by a Tukey HSD multiple comparisons test. The only significant difference was for acetate concentration among gut regions of *H. iris*, and those boxes sharing a letter are not statistically different from one another. Interspecific comparisons were made for each SCFA in each gut region individually with *t*-tests. Significant or marginally significant differences among the species are shown with brackets and the specific *P* value.

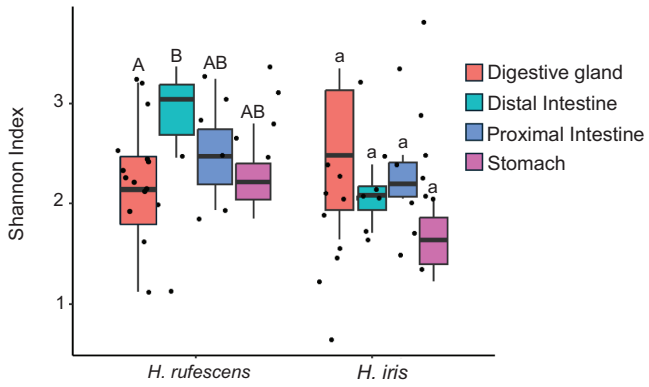

Figure 4. Box plot showing Shannon Diversity Index (α-diversity) of the microbial communities in the contents of various gut regions of the abalone species *Haliotis rufescens* and *Haliotis iris*. Intraspecific comparisons were made among gut regions with ANOVA. The only statistical difference was between the digestive gland and distal intestine of *H. rufescens*, as indicated with capital letters ($P = 0.05$). No differences were detected in *H. iris* ($P = 0.6$).

butyrate ($F_{2,33 = 3.103}$; $P = 0.0583$) concentrations (Fig. 3). In the stomach, *H. rufescens* had significantly higher acetate concentration than *H. iris* ($t = 2.203$, DF = 21, $P = 0.0389$), whereas propionate ($t = 0.243$, DF = 20, $P = 0.811$) did not differ. Like acetate, *H. rufescens* had higher stomach butyrate concentration than *H. iris* ($t = 2.353$, DF = 18.692, $P = 0.0297$). The two species were not different for acetate ($t = 0.649$, DF = 19, $P = 0.524$) or propionate ($t = 1.1665$, DF = 21, $P = 0.257$) concentrations in the proximal intestine, but *H. rufescens* did have significantly higher butyrate concentration than *H. iris* in this gut region ($t = 2.845$, DF = 21, $P = 0.010$). There were no differences in acetate ($t = 1.021$, DF = 19, $P = 0.320$), propionate ($t = 0.211$, DF = 16, $P = 0.835$), or butyrate ($t = 2.029$, DF = 21, $P = 0.055$) concentrations among the species in the distal intestine. The total SCFA concentrations in each gut region were as follows: *H. rufescens* stomach (average standard ± deviation) 5.54 ± 4.16 mM L^{-1}, proximal intestine 4.30 ± 2.31 mM L^{-1}, and distal intestine 2.98 ± 1.25 mM L^{-1}; *H. iris* stomach 2.22 ± 1.83 mM L^{-1}, proximal intestine 3.71 ± 2.12 mM L^{-1}, and distal intestine 2.92 ± 1.11 mM L^{-1}. No differences in total SCFA concentration were detected among gut regions for *H. rufescens* ($F_{2,33 = 0.884}$; $P = 0.423$) or *H. iris* ($F_{2,30 = 2.035}$; $P = 0.148$).

Microbiome Analyses

In terms of alpha diversity, the only difference detected for microbial communities of the contents of the abalone digestive systems was among the digestive glands and distal intestines of *Haliotis rufescens*, as no differences were detected for *Haliotis iris* (Fig. 4). For the gut tissue communities, *H. rufescens* showed no differences in alpha diversity among gut regions ($P > 0.47$ for any comparison; data not shown), whereas *H. iris* showed lower alpha diversity in its digestive gland than most tissues ($P < 0.05$ for each comparison; data not shown). Based on the PERMANOVA of the gut content community beta diversity ($P = 0.002$; $R^2 = 0.164$), gut region explained only 16% of the variation among the abalone species because host species itself was clearly the largest explanatory variable (Fig. 5). When examined individually by species, the gut region was not a significant predictor of microbial community in the gut contents of *H. rufescens* ($P = 0.160$, Fig. A1). Gut region, however, was a significant factor for the beta diversity of *H. iris* gut contents ($P = 0.006$,

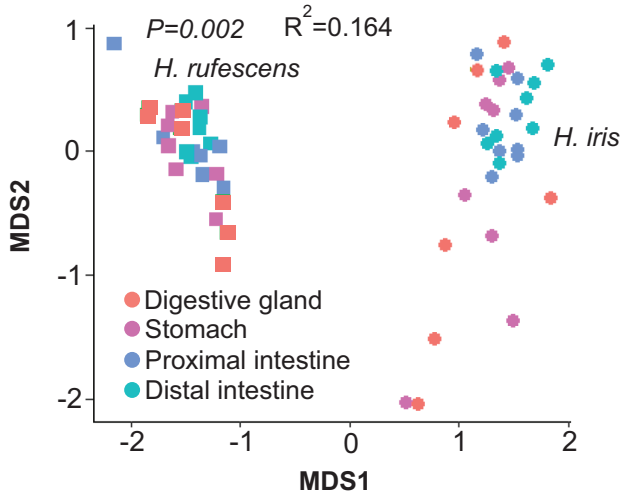

Figure 5. Nonmetric multidimensional scaling plot based on Bray–Curtis dissimilarity of the microbial communities in the contents of various gut regions of the abalone species *Haliotis rufescens* and *Haliotis iris*. Proximity to other symbols indicates similarity.

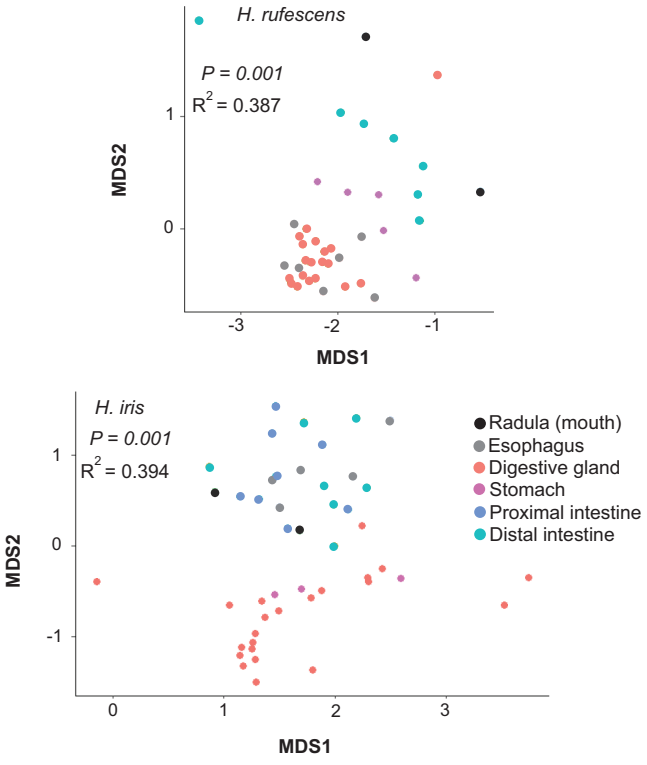

Figure 6. Nonmetric multidimensional scaling plots based on Bray–Curtis dissimilarity of the microbial communities in gut tissues of the abalone species *Haliotis rufescens* (top) and *H. iris* (bottom). Proximity to other symbols within a given graph indicates similarity. The results of PERMANOVA are displayed on the graphs. Note that there are no data for the proximal intestine of *H. rufescens*.

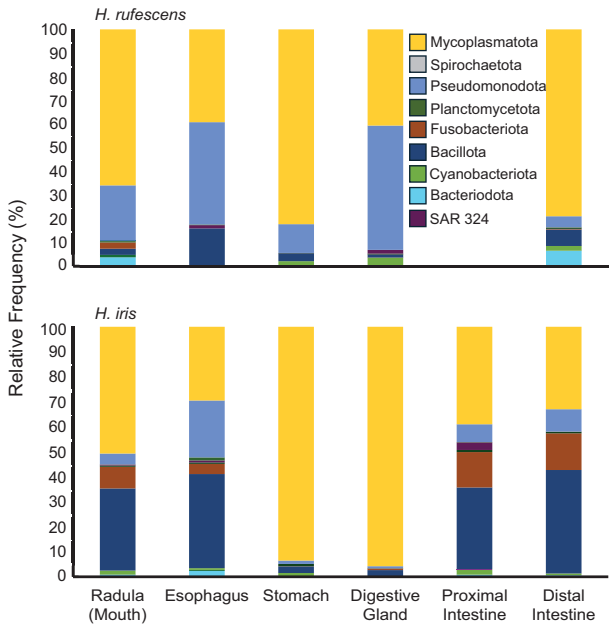

Figure 7. Stacked bar plots of the relative frequency of microbial communities (at the phylum level) in the gut tissues of different gut regions in the abalone species *Haliotis rufescens* and *Haliotis iris*. The key depicts the phyla. Note that we do not have data for the proximal intestine of *H. rufescens*. These phyla are also represented, but are too small to see (each representing <0.03%): Actinobacteriota, Campilobacterota, Chloroflexota, Desulfobacterota, Myxococcota, Verrucomicrobiota.

Fig. A1), with the distal intestine being different from the stomach ($P = 0.012$) and digestive gland ($P = 0.006$).

The beta diversity of the gut tissues showed strong differences among gut regions in both species, with gut region explaining about 39% of the variation in both species (Fig. 6). In *Haliotis rufescens*, the distal intestine tissue had different beta diversity from the stomach ($P = 0.003$) and digestive gland ($P = 0.003$). The radular (mouth) tissue community was also different from the stomach ($P = 0.045$) and digestive gland ($P = 0.044$; Fig. 6). In *Haliotis iris*, the stomach tissue community was different from the radula ($P = 0.018$), the proximal intestine ($P = 0.006$), and the distal intestine ($P = 0.004$). Similarly, the *H. Iris* digestive gland tissue community was different from the radula ($P = 0.004$), the proximal intestine ($P = 0.004$), and the distal intestine ($P = 0.004$). Differences in the tissue microbial communities are obvious among the gut regions in both species when viewed as stacked taxa bar plots (Fig. 7).

The most dominant bacterial phylum found in the abalone gut contents or tissues was the Mycoplasmatota, representing between 30% and 96% of all detected taxa depending on the sample type and gut region (Fig. 7, Fig. A2). The next most abundant phyla were the Pseudomonodota, Bacillota, Fusobacteriota, and Cyanobacteriota (Fig. 7, Fig. A2). A major difference between the two abalone species was in the phylum Bacillota, which was more abundant in *Haliotis iris* tissues than those of *Haliotis rufescens* (Fig. 7). There was an overwhelming dominance of Mycoplasmatota in the digestive gland and stomach tissues of *H. iris*, respresenting >95% and 93% of the sequences in these tissues, respectively (Fig. 7). In each abalone species, the indicator species analysis varied somewhat by gut region. For *H. rufescens* gut tissues, the mouth had indicator species in the Pseudomonodota (Gammaproteobacteria) and Bacteriodota (Flavobacteriaceae), whereas the esophagus, digestive gland, stomach, and intestinal tissues had more representation of Alphaproteobacteria (Pseudomonodota) and Mycoplasmatota as indicator species (Fig. 7, Supplemental Table S1). The esophogeal communities in *H. iris* had indicator species in the Pseudomonodota, Bacteriodota, Fusobacteriota, and Spirochaetota, whereas Mycoplasmatota took over as one traveled deeper into the *H. iris* gut (Fig. 7, Supplemental Table S1). In terms of the gut content communities, the distal intestines of *H. rufescens* and *H. iris* had Fusobacteriota (*Psychrilyobacter*), Mycoplasmatota (*Mycoplasma*), Pseudomonodota (*Vibrio*), and an unknown Bacteriodota as indicator species (Supplemental Table S2). Red abalone had *Francisella* (Pseudomonodota) and *H. iris* had an unknown Bacillota in their distal intestine contents as indicator species. *Haliotis iris* added in Verrucomicrobiota (Rubritaleaceae), Planctomycetota (Pirellulaceae), and Cyanobacteriota as indicator species in their digestive gland contents (Supplemental Table S1). The full microbial abundance data are in Supplemental Table S2.

DISCUSSION

In this study, digestive enzyme activities, concentrations of SCFAs, and the microbial communities in the guts of abalone species from the North (*Haliotis rufescens*) and South (*Haliotis iris*) Pacific Ocean were measured. Although the specific microbial taxa may vary among the host abalone species and ocean basins, the general representation on the phylum level looks a lot like other abalone from around the world, showing that abalone select and maintain a specific set of microbial taxa within their digestive systems in the wild or in captivity. That is, there is an "abalone microbiome" in comparison with seawater or other animals (e.g., Gobet et al. 2018). The stomach was hypothesized to have the highest microbial diversity and the highest SCFA concentrations along the abalone gut, and these hypotheses were soundly rejected. Although there was not as much variation in microbial taxa in the contents among the gut regions of the abalone species (Fig. 5), the microbial communities associated with the tissues of the various gut regions had more variation (Figs. 6 and 7), showing that microbial diversity is not homogenous along the abalone gut. There wasn't much variation in SCFA concentrations among the species, but the higher levels of butyrate found in *H. rufescens* in comparison with *H. iris* (Fig. 3) hints at some functional differences among their microbial communities. Overall, the digestive enzyme activities are generally in the same order of magnitude among the species, but *H. iris* may emphasize amylase, maltase, and acid phosphatase more so than *H. rufescens* (Fig. 2). Each of these observations will be discussed in more detail below.

Within the microbiome, members of the Mycoplasmatota (especially the genus *Mycoplasma*) dominated the gut tissue and content communities of *Haliotis rufescens* and *Haliotis iris*. This is an intriguing similarity, as these two abalone species occupy distinct habitats 10,800 km from each other across the ocean. Interestingly, Mycoplasmatota is a dominant phylum that is found across abalone species globally (Gobet et al. 2018, Nam et al. 2018, Choi et al. 2021, Cicala et al. 2023). Most examinations of abalone microbiomes are from farmed animals, so the similarity with wild abalone is of interest because

captivity impacts the enteric microbiomes of marine animals (Clements et al. 2014, Lavoie et al. 2018, Lavoie et al. 2021, Damasceno et al. 2022, Small et al. 2023).

Members of Mycoplasmatota (specifically in the genus *Mycoplasma*) are associated with a healthy gut in abalone (Cicala et al. 2023) and have a role in protecting host epithelium by inhibiting the binding of pathogens to the epithelial cells through competition for receptor sites (Villasante et al. 2020). In support of this, *Mycoplasma* abundance is typically high in healthy *Haliotis rufescens* and markedly decreases in abundance in individuals of this species that are infected with *Candidatus* Xenohaliotis californiensis, the causative bacteria of Withering Syndrome (Villasante et al. 2020). Of course, not all abalone species are exposed to *Candidatus* Xenohaliotis californiensis (as this bacterium is found on the West Coast of North American only) and the disease only appeared in the last several decades (Friedman et al. 2000, Crosson et al. 2014, Cicala et al. 2017), indicating that *Mycoplasma* likely has other important functional roles in the abalone gut. One such role may be in aiding healthy digestion, as members of the genus *Mycoplasma* have the capacity to digest nutrient-deplete food sources and supplement the host with simple carbohydrates and amino sugars (Villasante et al. 2020). In addition to *Mycoplasma*, Pseudomonodota (genus *Vibrio*) and Fusobacteriota (genus *Psychrilyobacter*) were also prevalent in the gut tissue of *H. rufescens* and *Haliotis iris*. These same genera are also commonly found in the intestines of *H. discus hannai* in Asia in the northwestern Pacific Ocean, and *Haliotis tuberculata* in Europe in the northeast Atlantic Ocean (Gobet et al. 2018, Yu et al. 2022, Liu et al. 2023), further indicating that abalone share core microbial taxa despite differing environmental conditions and physiologies. There is not much discussion of Cyanobacteriota in the abalone digestion literature, but there is indication that this phylum is prevalent in the tissues of other molluscs such as the oyster, *Crassostrea gigas*, with which they are likely symbionts (Avila-Poveda et al. 2014). Moreover, a prevalence of Cyanobacteriota was observed in *H. rufescens* fed different algal diets (Guo 2017). Their function or role in the abalone gut is unknown, but nonphotosynthetic Cyanobacteriota are gaining recognition as symbionts in herbivorous fish guts and are not just allochthonous bacteria consumed with algae (Soo et al. 2014, Pardesi et al. 2022) in comparison with photosynthetic cyanobacteria like *Synechococcus* sp., that are clearly environmental and more common in the gut contents than gut tissues (Fig. A2, Supplemental Table S2).

Although there were many similarities in the core microbial taxa between *Haliotis iris* and *Haliotis rufescens*, butyrate production is a key functional difference, with *H. rufescens* producing more butyrate than *H. iris* (Fig. 3). This is mirrored in the microbiome results, with *H. rufescens* also having a higher prevalence in Bacteroidota in their gut tissue versus *H. iris* (Fig. 7, Fig. A2). Members of the phylum Bacteroidota are known to produce SCFAs, like butyrate in human digestive systems (Shin et al. 2024), and are abundant in marine vertebrate species, such as green turtles (McDermid et al. 2020), and herbivorous fishes (Stevenson et al. 2022, Herrera et al. 2025). In these host species, Bacteroidota produce enzymes that can break down algal polysaccharides and ferment them into SCFAs, such as butyrate (Thomas et al. 2011, McDermid et al. 2020). Overall, the measured concentrations of SCFAs in the abalone digestive system (<30 mM L^{-1} total, let alone in a single gut region) suggest that abalone have some microbial fermentation occurring in their guts, but not on a level seen in some herbivorous fishes (Mountfort et al. 2002, Pardesi et al. 2022, Stevenson et al. 2022), and certainly not concentrated in the stomach, as hypothesized, suggesting that abalone are less reliant on microbial fermentation to digest their algal diet than some vertebrates. This is further matched by the relatively constant feeding and transit of material through the abalone gut, with transit times ranging between 12 and 20 h, possibly not long enough for high concentrations of SCFA to be achieved (Lyu et al. 2023).

Compartmentalization of the digestive system is common in invertebrates and vertebrates (Karasov & Douglas 2013). More voluminous regions of the gut (e.g., like a stomach or hindgut chamber) can slow transit times and allow for mixing, whereas tubular portions, like intestines, have plug-flow movement that tends to be more unidirectional (Penry & Jumars 1987, Horn & Messer 1992, Karasov & Douglas 2013, Lyu et al. 2023). Thus, finding differences in digestive enzyme activities and microbial communities among gut regions is to be expected, with microbes predicted to be more concentrated in voluminous regions (Penry 1989, Horn & Messer 1992, Harris et al. 1998, Garcia-Esquivel & Felbeck 2006, Nel et al. 2017, Pardesi et al. 2022, Sparagon et al. 2022, Lyu et al. 2023). Although higher microbial diversity and SCFA concentrations were not observed in the stomach, the indicator species analysis in this study revealed key microbial taxa that are more abundant in specific gut regions. For example, in the mouth tissue of *Haliotis rufescens*, members of Bacteroidota (family Flavobacteriacae) and Pseudomonodota (Gammaproteobacteria) were found to be indicator species. Members of Flavobacteriacae are known for the breakdown of algal polysaccharides (Li et al. 2017, Bäumgen et al. 2021), and Gammaproteobacteria are known in other abalone guts and produce alginate lyase that can break down alginate from brown algal cell walls (Yu et al. 2022).

When moving from the mouth to the esophagus and the remainder of the gut in *Haliotis rufescens*, the indicator species shift toward Alphaproteobacteria (Pseudomonodota) and *Mycoplasma*. Alphaproteobacteria have been associated with the digestive tissue of other abalone species, *Haliotis discus hannai* and *Haliotis gigantea* (Huang et al. 2020). For instance, a taxon closely related to *Thalassospira xiamenensis* (Alphaproteobacteria) was isolated from the digestive gland of *H. discus hannai* that had genes for alginate digestion and assimilation, suggesting this taxon may be involved in breaking down alginate from brown macroalgae (Huang et al. 2020). In comparison, the esophagus and remainder of the gut of *H. iris* contained Pseudomonodota, Bacillota, Bacteriodota, Fusobacteriota, and Spirochaetota. Members of Pseudomonodota are common in *H. discus hannai* intestines, as well as in the gut tissue of aquatic invertebrates more generally (Harris 1993, Yu et al. 2022). With *Vibrio* as the dominant genus out of the Psuedomonodota in many marine organisms (including abalone), they likely play a role in digestion (Hamid et al. 1979, MacDonald et al. 1986, Gatesoupe et al. 1997, Henderson & Millar 1998, Itoi et al. 2006, Ray et al. 2012, Egerton et al. 2018). *Psychrilyobacter* (Fusobacteriota) was also prevalent in the esophagus, which again indicates a role in digestion. This taxon has been found in the digestive tissue of *Haliotis tuberculata* and is known for fermenting simple sugars into SCFAs (Gobet et al. 2018, Yao et al. 2019). Detailed analyses of *Psychrilyobacter* isolated from *H. discus hannai* show

that it mostly metabolizes di- and monosaccharides, as opposed to polysaccharides (Liu et al. 2023). Lastly, Spirochaetota was an indicator species in the esophagus of *H. iris*. Members of this phylum have also been identified in the intestines of *H. discus hannai* and in species of freshwater snails (Yu et al. 2022, Apostolou et al. 2025). What these members of Spirochaetota do in the gut environment needs to be studied.

From a microbial perspective, it is obvious that the luminal gut content environment is different from the tissue mucosal environment in abalone (Fig. A2), as it is in fishes (Stevenson et al. 2022, Rankins et al. 2023, Herrera & German 2024). In their gut contents, *Haliotis rufescens* and *Haliotis iris* had shared taxa such as Fusobacteriota (*Psychrilyobacter*), Mycoplasmatota (*Mycoplasma*), Pseudomonodota (*Vibrio*), and an unknown Bacteriodota. Fusobacteria were also found in the intestines of *Haliotis discus hannai*, are known to produce enzymes that are critical for digestion, and aid in abalone digestion of marine algae (Parker-Graham et al. 2020, Guo et al. 2024). Unique to the distal intestine, *Francisella* sp. (Pseudomonodota) in *H. rufescens* and an unknown Bacillota in *H. iris*, were indicator species. This is interesting, as *Francisella* sp. infection can be pathogenic, and fatal, in *Haliotis gigantea* (Kamaishi et al. 2010), but the role of this species in *H. rufescens* is unknown.

This study is the first to examine the digestive microbiome of wild-collected *Haliotis rufescens* and *Haliotis iris*, providing an important baseline for future studies on digestion in these species. The results highlight similarities in bacterial taxa seen between *H. rufescens* and *H. iris* and among abalone more broadly, across varying culture conditions, environments, and physiologies. Moreover, the results strongly suggest that the abalone gut should not be treated as a single organ, but the different regions analyzed separately to discern the various functions along the gut (Garcia-Esquivel & Felbeck 2006). Further, there are differences in the communities among the gut contents and tissues, which should be accounted for.

The use of programs like PICRUSt2, whereas improving in utility for predicting the functional roles of microbes in vertebrate studies (particularly in mammals), are risky in unknown environments (Langille et al. 2013, Abushattal et al. 2020), like the guts of abalone, because strain variants can differ in function depending on environment (Shade et al. 2012, Sunagawa et al. 2015). Future studies should incorporate several "omics" approaches, including metagenomics and transcriptomics (Nam et al. 2018), proteomics (Starr et al. 2018), and metabolomics (Sparagon et al. 2022) to further understand microbial functions within the abalone guts.

A consistent result in this study is the higher amylase and maltase activities in the guts of *Haliotis iris* in comparison with *Haliotis rufescens* (Fig. 3, Table 1). Because of the evolutionary and habitat differences among the two species, it is difficult to point to a specific reason for the elevated ability to digest and assimilate soluble starches in *H. iris*, but amylase (not maltase) was also more elevated in laboratory-reared *H. iris* relative to *H. rufescens* in a previous experiment suggesting that this may be consistent difference among the species (Frederick et al. 2022). Again, this is not just a temperature difference in the assays used in this study (12 versus 14°C), as *H. iris* consistently had elevated amylase over *H. rufescens* regardless of temperature (Frederick et al. 2022), perhaps pointing to differences in nutrient content of algae consumed 10,800 km apart (e.g., Whyte & Englar 1978, Smith et al. 2010, Battershill 2024, Hrstich-Manning & Aguirre 2025). Similarly, alanine aminopeptidase activities are absent from *H. iris*, but clearly measurable in *H. rufescens*. Pāua may make up for this with more elevated leucine aminopeptidase activities (Fig. 2, Table 1). Why *H. iris* lacks an alanine aminopeptidase requires further investigation. Is that a function of that species or the clade to which they belong? Trypsin activity was measured at pH 7.0 in the digestive gland samples, which makes sense, seeing that the substrate used (BAPNA) is not stable at pH values below 7.0 (Preiser et al. 1975). Abalone do have proteases that operate under more acidic conditions in their digestive glands (Picos-García et al. 2000) and future work should use dissolved protein assays (Anson 1938) as opposed to colorimetric substrates that provide more flexibility of assay conditions.

The acid phosphatase activities in *Haliotis iris* are two orders of magnitude higher than those in *Haliotis rufescens*. Acid phosphatase can be indicative of immune function (Singh et al. 2020, Singh & Lin 2021, Bullon et al. 2023) as well as nutrient processing rates (Yoshida et al. 1977, Harpaz & Uni 1999, Carneiro et al. 2020, Fronte et al. 2021) in fishes and abalone. Because these are wild animals, there could be differences in phosphate availability among the algae consumed and/or locations that could explain this difference. For example, *Ecklonia* (common in the *H. iris* diet) has double the phosphate of *Macrocystis* (Smith et al. 2010), the latter of which being more common in the *H. rufescens* diet and having relatively stable and lower phosphate concentrations over time (Whyte & Englar 1978). Hence, with more phosphate in the diet, *H. iris* may invest more in acid phosphatase expression. Many digestive enzyme activity differences involve differences in gene copy number. A classic example is that of amylase among fish species with different diets, with those fish consuming more starch having more amylase gene copies and elevated amylase activity that can be orders of magnitude higher than species consuming low-starch diets with fewer amylase genes (German et al. 2016, Heras et al. 2020, Le et al. 2023). Variations of this magnitude are unknown for acid phosphatase, however, and deserve more attention here. There is a genome for *H. rufescens* (Masonbrink et al. 2019), but not for *H. iris*, making such a comparison impossible at this time. All of this is offered with the caveat that *H. iris* fed *Ecklonia* and *Lessonia* in the laboratory did not show the elevated acid phosphatase seen in the wild animals in this study (Frederick et al. 2022). Thus, it may be more of an environmental difference issue than something purely dietary or adaptive among the species. Furthermore, this gets at a limitation of a two-species comparison. One cannot point at any one variable to explain differences among the species. Therefore, this leads to a call for more studies of gut physiology and microbiomes of wild abalone, using closely-related species that are sympatric so that the impacts of diet and environment can be separated from those driven by phylogenetic history (e.g., German et al. 2004, German et al. 2010, German et al. 2015).

CONCLUSION

Management of abalone must be grounded in a biological knowledge of the species involved. Although limited as a two-species comparison, this work improves the understanding of the digestive physiological functions of two important abalone species in their native habitat on a natural diet. This work can be used as a baseline to understand changes in physiological function that occur during a shift from wild-caught

fisheries to farmed abalone. Conserved patterns among these two species (e.g., *Mycoplasma* being a dominant genus in the microbiome) leads to an expectation of similar patterns in some of the critically endangered abalone species, such as white abalone (*Haliotis sorenseni)* and black abalone (*Haliotis cracherodii*) in North America. For instance, the White Abalone Captive Breeding Program relies heavily on applying physiological data from related species to the critically endangered white abalone restoration aquaculture practices. Is the dominance of Pseudomonodota seen in the guts of *H. sorenseni* in captivity (Parker-Graham et al. 2020) an indication of poor animal health, an inadequate diet, a unique signature of this species, or some bioinformatic methodological difference among that study and others? The current work here certainly provides impetus for more work on endangered *H. sorenseni* to better understand their digestion, microbiome, and how to best raise them for species recovery. As wild abalone populations decline across the world, it is crucial to preserve a baseline understanding of their physiology within their native habitats, and this paper provides that for two iconic abalone species.

AUTHOR CONTRIBUTIONS

Conceptualization: A. L., A. R. F., and D. P. G. Methodology, A. L., A. R. F., and D. P. G. Investigation: A. L., A. R. F., M. J. H., and L. A. Writing-original draft: A. L., A. R. F., L. A., D. P. G. Writing-reviewing and editing: A. L., L. A., M. J. H., A. R. F., and D. P. G.

DATA ACCESSIBILITY

All data are presented within the manuscript, figures, supplemental material associated with this manuscript, or online at: https://german.bio.uci.edu/Supplements.html

DECLARATION OF COMPETING INTERESTS

The authors have no conflicts of interest to declare that are relevant to the content of this article.

FUNDING

This work was supported by a National Geographic Young Explorers Grant to ARF [Grant No. CP-054ER-17], a University of California Irvine (UCI) OCEANS Graduate Student Fellowship (ARF); UCI Newkirk Center for Science and Society (ARF); the Western Society of Malacologists Research Grant (ARF); the National Science Foundation Graduate Research Fellowship to ARF [Grant No. DGE- 1321846], a UCI Microbiome Initiative Grant (to ARF), and the UCI Undergraduate Research Opportunity Program (to A. L.).

ACKNOWLEDGMENTS

The work presented here was conducted primarily on the occupied and unceded land of the Tongva and Acjachemen Nations, for whom abalone are incredibly important. The authors acknowledge that they and their work have benefited and continue to benefit from access to this land and the denial of these Nations and Tangata whenua from their traditional territories. The word abalone comes from Rumsen, a Constanoan language traditionally spoken in what is now called the Monterey Bay area. We deeply thank the red abalone fishers who donated the guts of their catches to our work: T. J. Isley, K. P. Umbarger, B. M. Perlman, A. N. Peterson, and P. L. Braciszewski. We would also like to acknowledge the Wellington University Coastal Ecology Laboratory at the Victoria University of Wellington (Aotearoa New Zealand), for providing space to dissect animals and for collecting animals for this work, especially John Van der Sman, Daniel McNaughtan, and Dan Crossett (Cawthron).

LITERATURE CITED

Abushattal, S., A. Vences, A. V. Barca & C. R. Osorio. 2020. Diverse horizontally-acquired gene clusters confer sucrose utilization to different lineages of the marine pathogen *photobacterium damselae* subsp. *Genes (Basel)*. 11:1244.

Ansary, M. W. R., H. S. Jeong, K. W. Lee, H. S. Kim, J. Kim, A. Yun, S. H. Cho, P. Y. Kim & T.-I. Kim. 2019. The effect of substituting *Undaria pinnatifida* in formulated feeds with *Sargassum horneri* on growth and body composition of juvenile abalone (*Haliotis discus*, Reeve 1846). *J. Appl. Phycol.* 31:2125–2132.

Anson, M. L. 1938. The estimation of pepsin, trypsin, papain, and cathepsin with hemoglobin. *J. Gen. Physiol.* 22:79–89.

Apostolou, K., C. Radea, A. Meziti & K. A. Kormas. 2025. Bacterial diversity associated with terrestrial and aquatic snails. *Microorganis.* 13:8.

Avila-Poveda, O. H., A. Torres-Ariño, D. A. Girón-Cruz & A. Cuevas-Aguirre. 2014. Evidence for accumulation of *Synechococcus elongatus* (Cyanobacteria: Cyanophyceae) in the tissues of the oyster *Crassostrea gigas* (Mollusca: Bivalvia). *Tissue Cell.* 46:379–387.

Axelsson, E., A. Ratnakumar, M. L. Arendt, K. Maqbool, M. T. Webster, M. Perloski, O. Liberg, J. M. Arnemo, A. Hedhammar & K. Lindblad-Toh. 2013. The genomic signature of dog domestication reveals adaptation to a starch-rich diet. *Nature.* 495:360–364.

Bansemer, M. S., J. G. Qin, J. O. Harris, D. N. Duong, T. H. Hoang, G. S. Howarth & D. A. J. Stone. 2016. Growth and feed utilisation of greenlip abalone (*Haliotis laevigata*) fed nutrient enriched macroalgae. *Aquacult.* 452:62–68.

Bansemer, M. S., J. G. Qin, J. O. Harris, E. N. Schaefer, H. Wang, G. J. Mercer, G. S. Howarth & D. A. J. Stone. 2016. Age-dependent response of digestive enzyme activities to dietary protein level and water temperature in greenlip abalone (*Haliotis laevigata*). *Aquacult.* 451:451–456.

Battershill, Z. V. 2024. Nutritional profiling of five New Zealand seaweeds – a preliminary assessment. *Front. Mar. Sci.* 11:1410005.

Bäumgen, M., T. Dutschei & U. T. Bornscheuer. 2021. Marine polysaccharides: occurrence, enzymatic degradation and utilization. *Chembiochem.* 22:2247–2256.

Bullon, N., A. Seyfoddin & A. C. Alfaro. 2023. The role of aquafeeds in abalone nutrition and health: a comprehensive review. *J. World Aquaculture Soc.* 54:7–31.

California Department of Fish and Wildlife. 2005. Abalone Recovery And Management Plan (ARMP). Sacramento, CA: California Department of Fish and Wildlife.

Caporaso, J. G., C. L. Lauber, W. A. Walters, D. Berg-Lyons, J. Huntley, N. Fierer, S. M. Owens, J. Betley, L. Fraser, M. Bauer, N. Gormley, J. A. Gilbert, G. Smith & R. Knight. 2012. Ultra-high-throughput microbial community analysis on the Illumina HiSeq and Miseq platforms. *ISME J.* 6:1621–1624.

Carneiro, W. F., T. F. D. Castro, T. M. Orlando, F. Meurer, D. A. J. Paula, B. C. R. Virote, A. R. C. B. Vianna & L. D. S. Murgas. 2020. Replacing fish meal by chlorella sp. Meal: effects on zebrafish growth, reproductive performance, biochemical parameters and digestive enzymes. *Aquacult.* 528:735612.

Choi, M.-J., D. O. Young, Y. R. Kim, J. K. Lim & J.-M. Kim. 2021. Intestinal microbial diversity is higher in Pacific abalone (*Haliotis discus hannai*) with slower growth rates. *Aquacult.* 537:736500.

Cicala, F., J. A. Cisterna-Céliz, M. Paolinelli, J. D. Moore, J. Sevigny & A. Rocha-Olivares. 2023. The role of diversity in mediating microbiota structural and functional differences in two sympatric species of abalone under stressed withering syndrome conditions. *Microb. Ecol.* 85:277–287.

Cicala, F., J. D. Moore, J. Cáceres-Martínez, M. A. Del Río-Portilla, M. Hernández-Rodríguez, R. Vásquez-Yeomans & A. Rocha-Olivares. 2017. Multigenetic characterization of '*Candidatus Xenohaliotis californiensis*'. *Int J Systemat Evol Microbiol.* 67:42–49.

Clements, K. D., E. R. Angert, W. L. Montgomery & J. H. Choat. 2014. Intestinal microbiota in fishes: what's known and what's not. *Mol. Ecol.* 23:1891–1898.

Coleman, A. W. & V. D. Vacquier. 2002. Exploring the phylogenetic utility of ITS sequences for animals: a test case for abalone (Haliotis). *J. Mol. Evol.* 54:246–257.

Cornwall, C. E., N. E. Phillips & D. C. McNaught. 2009. Feeding preferences of the abalone *Haliotis iris* in relation to macroalgal species, attachment, accessibility and water movement. *J Shellfish Res.* 28:589–597. 589.

Crosson, L. M., N. Wight, G. R. VanBlaricom, I. Kiryu, J. D. Moore & C. S. Friedman. 2014. Abalone withering syndrome: distribution, impacts, current diagnostic methods and new findings. *Dis. Aquat. Organ.* 108:261–270.

Damasceno, M. R. A., C. G. d C. Lemes, L. S. S. B. Braga, P. C. Tizioto, H. Montenegro, M. Paduan, J. G. Pereira, I. F. Cordeiro, L. C. M. Rocha, S. A. da Silva, A. B. Sanchez, W. G. Lima, G. M. Yazbeck, L. M. Moreira & C. C. M. Garcia. 2022. Hatchery tanks induce intense reduction in microbiota diversity associated with gills and guts of two endemic species of the São Francisco River. *Front. Microbiol.* 13:966436.

De Cáceres, M., P. Legendre, S. K. Wiser & L. Brotons. 2012. Using species combinations in indicator value analyses. *Methods Ecol. Evol.* 3:973–982.

Degliesposti, M., S. Devries, M. Crimi, A. Ghelli, T. Patarnello & A. Meyer. 1993. Mitochondrial cytochrome-B: evolution and structure of the protein. *Biochim Biophys Acta.* 1143:243–271.

Egerton, S., S. Culloty, J. Whooley, C. Stanton & R. P. Ross. 2018. The gut microbiota of marine fish. *Front. Microbiol.* 9:873.

Erasmus, J. H., P. A. Cook & V. E. Coyne. 1997. The role of bacteria in the digestion of seaweed by the abalone *Haliotis midae*. *Aquacult.* 155:377–386.

Estes, J. A., D. R. Lindberg & C. Wray. 2005. Evolution of large body size in abalones (*haliotis*): patterns and implications. *Paleobiol.* 31:591–606.

Frederick, A. R. 2019. How do warming temperatures and disease affect abalone? Examining digestive physiology and withering syndrome in *Haliotis*. Doctoral dissertation, Biological Sciences, University of California, Irvine. p. 120.

Frederick, A. R., A. M. Lee, B. A. Wehrle, C. C. Catabay, D. R. Rankins, K. D. Clements & D. P. German. 2022. Abalone under moderate heat stress have elevated metabolic rates and changes to digestive enzyme activities. *Comp. Biochem. Physiol. A Mol. Integr. Physiol.* 270:111230.

Friedman, C. S., K. B. Andree, K. A. Beauchamp, J. D. Moore, T. T. Robbins, J. D. Shields & R. P. Hedrick. 2000. *Candidatus* xenohaliotis californiensis, a newly described pathogen of abalone, *haliotis* spp., along the west coast of North America. *Int. J. Syst. Evol. Microbiol.* 50 Pt 2:847–855.

Fronte, B., R. Licitra, C. Bibbiani, L. Casini, M. De Zoysa, V. Miragliotta, S. Sagona, F. Coppola, L. Brogi & F. Abramo. 2021. Fishmeal replacement with *Hermetia illucens* meal in aquafeeds: effects on zebrafish growth performances, intestinal morphometry, and enzymology. *Fishes.* 6:28.

Garcia-Esquivel, Z. & H. Felbeck. 2006. Activity of digestive enzymes along the gut of juvenile red abalone, *Haliotis rufescens*, fed natural and balanced diets. *Aquacult.* 261:615–625.

Gatesoupe, F.-J., J.-L. Z. Infante, C. L. Cahu & P. Quazuguel. 1997. Early weaning of seabass larvae, *Dicentrarchus labrax*: the effect on microbiota, with particular attention to iron supply and exoenzymes. *Aquacult.* 158:117–127.

Geiger, D. L. & B. Owen. 2012. Abalone: world-wide haliotidae. Hackenheim, Germany: Conchbooks.

German, D. P., D. M. Foti, J. Heras, H. Amerkhanian & B. L. Lockwood. 2016. Elevated gene copy number does not always explain elevated amylase activities in fishes. *Physiol. Biochem. Zool.* 89:277–293.

German, D. P., M. H. Horn & A. Gawlicka. 2004. Digestive enzyme activities in herbivorous and carnivorous prickleback fishes (Teleostei: Stichaeidae): ontogenetic, dietary, and phylogenetic effects. *Physiol. Biochem. Zool.* 77:789–804.

German, D. P., B. C. Nagle, J. M. Villeda, A. M. Ruiz, A. W. Thomson, S. Contreras-Balderas & D. H. Evans. 2010. Evolution of herbivory in a carnivorous clade of minnows (Teleostei: Cyprinidae): effects on gut size and digestive physiology. *Physiol. Biochem. Zool.* 83:1–18.

German, D. P., A. Sung, P. K. Jhaveri & A. Agnihotri. 2015. More than one way to be an herbivore: convergent evolution of herbivory using different digestive strategies in prickleback fishes (family stichaeidae). *Zoology (Jena).* 118:161–170.

Gobet, A., L. Mest, M. Perennou, S. M. Dittami, C. Caralp, C. Coulombet, S. Huchette, S. Roussel, G. Michel & C. Leblanc. 2018. Seasonal and algal diet-driven patterns of the digestive microbiota of the European abalone *Haliotis tuberculata*, a generalist marine herbivore. *Microbiome.* 6:60.

Gómez-Pinchetti, J. L. & G. García-Reina. 1993. Enzymes from marine phycophages that degrade cell walls of seaweeds. *Mar Biol.* 116:553–558.

Guo, J. C. 2017. Metabarcoding analyses of gut microbiome compositions in red abalone (*Haliotis rufescens*, Swainson, 1822) fed different macroalgal diets. Master's thesis, Marine Science, California State University Monterey Bay. p. 77.

Guo, Z., X. Hou, L. Chang, Z.-J. Du, K. Shi, A. Song, Z. Liang & J. Gu. 2024. Effects of different feeding patterns on growth, enzyme activity, and intestinal microbiome of the juvenile Pacific abalone *Haliotis discus hannai*. *Aquacult Rep.* 39:102427.

Hamid, A., T. Sakata & D. Kakimoto. 1979. Microflora in the alimentary tract of gray mullet-iv estimation of enzymic activities of the intestinal bacteria. *Nipp Suis Gakki.* 45:99–106.

Harpaz, S. & Z. Uni. 1999. Activity of intestinal mucosal brush border membrane enzymes in relation to the feeding habits of three aquaculture fish species. *Comp Biochem Physiol A.* 124:155–160.

Harris, J. M. 1993. The presence, nature, and role of gut microflora in aquatic invertebrates: a synthesis. *Microb. Ecol.* 25:195–231.

Harris, J. O., C. M. Burke & G. B. Maguire. 1998. Characterization of the digestive tract of greenlip abalone, *Haliotis laevigata* Donovan. II. Microenvironment and bacterial flora. *J Shellfish Res.* 17:989–994.

Henderson, R. J. & R. M. Millar. 1998. Characterization of lipolytic activity associated with a *vibrio* species of bacterium isolated from fish intestines. *J. Mar. Biotechnol.* 6:168–173.

Heras, J., M. Chakraborty, J. J. Emerson & D. P. German. 2020. Genomic and biochemical evidence of dietary adaptation in a marine herbivorous fish. *Proc. Biol. Sci.* 287:20192327.

Herrera, M. J. & D. P. German. 2024. Intestinal microbiome function. In: S. L. Alderman & T. E. Gillis, editors. Encyclopedia of fish physiology, 2nd edition, Oxford: Academic Press. pp. 419–430.

Herrera, M. J., J. Heras, C. Catabay, M. T. Booth, K. M. Connor & D. P. German. 2025. Diet-induced shifts in the hindgut microbiome leads to subtle changes in gut and liver function of a marine herbivorous fish. *Ecol. Evol. Physiol.* 98:111–131.

Horn, M. H. & K. S. Messer. 1992. Fish guts as chemical reactors: a model for the alimentary canals of marine herbivorous fishes. *Mar Biol.* 113:527–535.

Hrstich-Manning, G. & J. D. Aguirre. 2025. Nutritional composition of common, coastal seaweeds from northeastern New Zealand. *New Zealand J Mar Freshwat Res.* 59:485–500.

Huang, Z., J. M. Petersen, J. Martijn, T. J. G. Ettema & Z. Shao. 2020. A novel alphaproteobacterium with a small genome identified from the digestive gland of multiple species of abalone. *Environ. Microbiol. Rep.* 12:387–395.

Hur, S.-W., J. Cadangin, S. Lee, J.-H. Lee, S.-J. Park, W.-J. Jang & Y.-H. Choi. 2023. Dietary replacement of *Undaria pinnatifida* by *Sargassum horneri* in feed formulation for abalone *Haliotis discus hannai:* effect on growth, gut microbiota, and taste sensory profile. *Front. Mar. Sci.* 10:

Iehata, S., T. Inagaki, S. Okunishi, M. Nakano, R. Tanaka & H. Maeda. 2009. Colonization and probiotic effects of lactic acid bacteria in the gut of the abalone *Haliotis gigantea*. *Fish. Sci.* 75:1285–1293.

Iehata, S., T. Inagaki, S. Okunishi, M. Nakano, R. Tanaka & H. Maeda. 2010. Improved gut environment of abalone *Haliotis gigantea* through *Pediococcus* sp. Ab1 treatment. *Aquacult.* 305:59–65.

Itoi, S., T. Okamura, Y. Koyama & H. Sugita. 2006. Chitinolytic bacteria in the intestinal tract of Japanese coastal fishes. *Can. J. Microbiol.* 52:1158–1163.

Kamaishi, T., S. Miwa, E. Goto, T. Matsuyama & N. Oseko. 2010. Mass mortality of giant abalone *Haliotis gigantea* caused by a *Francisella* sp. bacterium. *Dis. Aquat. Organ.* 89:145–154.

Karasov, W. H. 1992. Tests of the adaptive modulation hypothesis for dietary control of intestinal nutrient transport. *Am. J. Physiol.* 263:R496–R502.

Karasov, W. H. & A. E. Douglas. 2013. Comparative digestive physiology. *Comprehens Physiol.* 3:741–783.

Karasov, W. H., K. D. Kohl & E. Caviedes-Vidal. 2025. The dynamic gut: the vertebrate gastrointestinal tract and associated microbiome exhibit physiological flexibility and adaptations to diet. *J Exp Biol.* 228:250395.

Karasov, W. H. & C. Martínez del Rio. 2007. Physiological ecology: How animals process energy, nutrients, and toxins. Princeton, NJ: Princeton University Press.

Kim, K. H., M. H. Horn, A. E. Sosa & D. P. German. 2014. Sequence and expression of an alpha-amylase gene in four related species of prickleback fishes (Teleostei: Stichaeidae): ontogenetic, dietary, and species-level effects. *J. Comp. Physiol. B.* 184:221–234.

Langille, M. G. I., J. R. Zaneveld, J. G. Caporaso, D. McDonald, D. Knights, J. A. Reyes, J. C. Clemente, D. E. Burkepile, R. L. Vega Thurber, R. Knight, R. G. Beiko & C. Huttenhower. 2013. Predictive functional profiling of microbial communities using 16s rRNA marker gene sequences. *Nat. Biotechnol.* 31:814–821.

Lavoie, C., M. Courcelle, B. Redivo & N. Derome. 2018. Structural and compositional mismatch between captive and wild Atlantic salmon (*Salmo salar*) parrs' gut microbiota highlights the relevance of integrating molecular ecology for management and conservation methods. *Evol. Appl.* 11:1671–1685.

Lavoie, C., K. Wellband, A. Perreault, L. Bernatchez & N. Derome. 2021. Artificial rearing of Atlantic salmon juveniles for supportive breeding programs induces long-term effects on gut microbiota after stocking. *Microorganism.* 9:1932.

Le, N., J. Heras, M. J. Herrera, D. P. German & L. T. Crummett. 2023. The genome of *Anoplarchus purpurescens* (Stichaeidae) reflects its carnivorous diet. *Mol. Genet. Genomics.* 298:1419–1434.

Lee, Y. & V. D. Vacquier. 1992. The divergence of species-specific abalone sperm lysins is promoted by positive Darwinian selection. *Biol. Bull.* 182:97–104.

Leigh, S. C., Y. P. Papastamatiou & D. P. German. 2021. Gut microbial diversity and digestive function of an omnivorous shark. *Mar. Biol.* 168:55.

Leighton, D. L. 2000. The biology and culture of the California abalones. Pittsburgh, PA: Dorrance Publishing Company.

Li, M., Q. Shang, G. Li, X. Wang & G. Yu. 2017. Degradation of marine algae-derived carbohydrates by bacteroidetes isolated from human gut microbiota. *Mar Drug.* 15:92.

Li, W., H. Cao, W. Xu, M. Mahmood, W. Ahmed, S. Mehmood & W. You. 2023. An analysis of the cloning, functional analysis, and identification of three cloned digestive enzymes associated with growth traits in *Haliotis diversicolor*. *Aquacult Res.* 2023:1–14.

Liu, M., G. Wei, Q. Lai, Z. Huang, M. Li & Z. Shao. 2023. Genomic and metabolic insights into the first host-associated isolate of *psychrilyobacter*. *Microbiol. Spectr.* 11:e03990-03922.

Lyu, M., X. Gao, M. Zhang, S. Lin & C. Ke. 2023. Circadian feeding characteristics of different abalone species and construction of a gastrointestinal evacuation model. *Aquacult.* 576:739826.

MacDonald, N. L., J. R. Stark & B. Austin. 1986. Bacterial microflora in the gastro-intestinal tract of dover sole (*Solea solea* l.), with emphasis on the possible role of bacteria in the nutrition of the host. *FEMS Microbiol Lett.* 35:107–111.

Masonbrink, R. E., C. M. Purcell, S. E. Boles, A. Whitehead, J. R. Hyde, A. S. Seetharam & A. J. Severin. 2019. An annotated genome for *Haliotis rufescens* (red abalone) and resequenced green, pink, pinto, black, and white abalone species. *Genome Biol. Evol.* 11:431–438.

McDermid, K. J., R. P. Kittle, A. Veillet, S. Plouviez, L. Muehlstein & G. H. Balazs. 2020. Identification of gastrointestinal microbiota in Hawaiian green turtles (*Chelonia mydas*). *Evol Bioinformat.* 16:1176934320914603.

Mountfort, D., J. Campbell & K. D. Clements. 2002. Hindgut fermentation in three species of marine herbivorous fish. *Appl. Environ. Microbiol.* 68:1374–1380.

Nam, B.-H., J. Jang, K. Caetano-Anolles, Y.-O. Kim, J. Y. Park, H. Sohn, S. H. Yoon, H. Kim & W. Kwak. 2018. Microbial community and functions associated with digestion of algal polysaccharides in the visceral tract of *Haliotis discus hannai*: insights from metagenome and metatranscriptome analysis. *PLoS One.* 13:e0205594–13.

Nam, B.-H., W. Kwak, Y.-O. Kim, D.-G. Kim, H. J. Kong, W.-J. Kim, J.-H. Kang, J. Y. Park, C. M. An, J.-Y. Moon, C. J. Park, J. W. Yu, J. Yoon, M. Seo, K. Kim, D. K. Kim, S. Lee, S. Sung, C. Lee, Y. Shin, M. Jung, B.-C. Kang, G.-H. Shin, S. Ka, K. Caetano-Anolles, S. Cho & H. Kim. 2017. Genome sequence of Pacific abalone (*Haliotis discus hannai*): the first draft genome in family Haliotidae. *Gigascience.* 6:1–8.

Naylor, R. L., R. W. Hardy, A. H. Buschmann, S. R. Bush, L. Cao, D. H. Klinger, D. C. Little, J. Lubchenco, S. E. Shumway & M. Troell. 2021. A 20-year retrospective review of global aquaculture. *Nature.* 591:551–563.

Nel, A., B. I. Pletschke & P. J. Britz. 2017. The effect of low-level kelp supplementation on digestive enzyme activity levels in cultured abalone *Haliotis midae* fed formulated feeds. *Afr J Mar Sci.* 39:179–182.

Pardesi, B., A. M. Roberton, K. C. Lee, E. R. Angert, D. I. Rosendale, S. Boycheva, W. L. White & K. D. Clements. 2022. Distinct microbiota composition and fermentation products indicate functional compartmentalization in the hindgut of a marine herbivorous fish. *Mol. Ecol.* 31:2494–2509.

Parker-Graham, C. A., A. Eetemadi, Z. Yazdi, B. C. Marshman, M. Loeher, C. A. Richey, S. Barnum, J. D. Moore & E. Soto. 2020. Effect of oxytetracycline treatment on the gastrointestinal microbiome of critically endangered white abalone (*Haliotis sorenseni*) treated for withering syndrome. *Aquacult.* 526:735411.

Penry, D. L. 1989. Tests of kinematic models for deposit-feeders' guts: patterns of sediment processing by *Parastichopus californicus* (Stimpson) (Holothuroidea) and *Amphicteis scaphobranchiata* Moore (Polychaeta). *J Exp Mar Biol Ecol.* 128:127–146.

Penry, D. L. & P. A. Jumars. 1987. Modeling animal guts as chemical reactors. *Am Nat.* 129:69–96.

Perry, G. H., N. J. Dominy, K. G. Claw, A. S. Lee, H. Fiegler, R. Redon, J. Werner, F. A. Villanea, J. L. Mountain, R. Misra, N. P. Carter, C. Lee & A. C. Stone. 2007. Diet and the evolution of human amylase gene copy number variation. *Nat. Genet.* 39:1256–1260.

Picos-García, C., F. L. García-Carreño & E. Serviere-Zaragoza. 2000. Digestive proteases in juvenile Mexican green abalone, *Haliotis fulgens*. *Aquacult.* 181:157–170.

Preiser, H., J. Schmitz, D. Maestracci & R. K. Crane. 1975. Modification of an assay for trypsin and its application for the estimation of enteropeptidase. *Clin. Chim. Acta.* 59:169–175.

Pryor, G. S. & K. Bjorndal. 2005. Symbiotic fermentation, digesta passage, and gastrointestinal morphology in bullfrog tadpoles (*Rana catesbeiana*). *Physiol. Biochem. Zool.* 78:201–215.

Quast, C., E. Pruesse, P. Yilmaz, J. Gerken, T. Schweer, P. Yarza, J. Peplies & F. O. Glöckner. 2012. The SILVA ribosomal RNA gene database project: improved data processing and web-based tools. *Nucleic Acids Res.* 41:D590–D596.

R. Core Team. 2020. R: A language and environment for statistical computing. Vienna, Austria: R Foundation for Statistical Computing.

Rankins, D. R., M. J. Herrera, M. P. Christensen, A. Chen, N. Z. Hood, J. Heras & D. P. German. 2023. When digestive physiology doesn't match "diet": *Lumpenus sagitta* (stichaeidae) is an "omnivore" with a carnivorous gut. *Comp. Biochem. Physiol. A Mol. Integr. Physiol.* 285:111508.

Ray, A. K., K. Ghosh & E. Ringø. 2012. Enzyme-producing bacteria isolated from fish gut: a review. *Aquacult Nutr.* 18:465–492.

Ronquist, F., M. Teslenko, P. van der Mark, D. L. Ayres, A. Darling, S. Hohna, B. Larget, L. Liu, M. A. Suchard & J. P. Huelsenbeck. 2012. MrBayes 3.2: efficient Bayesian phylogenetic inference and model choice across a large model space. *Syst. Biol.* 61:539–542.

Sawabe, T., N. Setoguchi, S. Inoue, R. Tanaka, M. Ootsubo, M. Yoshimizu & Y. Ezura. 2003. Acetic acid production of *Vibrio halioticoli* from alginate: a possible role for establishment of abalone–*v. Halioticoli* association. *Aquacult.* 219:671–679.

Schiel, D. R., N. L. Andrew & M. S. Foster. 1995. The structure of subtidal algal and invertebrate assemblages at the Chatham Islands, New Zealand. *Mar Biol.* 123:355–367.

Schiel, D. R. & P. A. Breen. 1991. Population structure, ageing, and fishing mortality of the New Zealand abalone *Haliotis iris*. *Fish Bull, U.S.* 89:681–691.

Shade, A., H. Peter, S. D. Allison, D. L. Baho, M. Berga, H. Bürgmann, D. H. Huber, S. Langenheder, J. T. Lennon, J. B. H. Martiny, K. L. Matulich, T. M. Schmidt & J. Handelsman. 2012. Fundamentals of microbial community resistance and resilience. *Front. Microbiol.* 3:417.

Shin, J. H., G. Tillotson, T. N. MacKenzie, C. A. Warren, H. M. Wexler & E. J. C. Goldstein. 2024. Bacteroides and related species: the keystone taxa of the human gut microbiota. *Anaerob.* 85:102819.

Singh, S. B., A. Carroll-Portillo, C. Coffman, N. L. Ritz & H. C. Lin. 2020. Intestinal alkaline phosphatase exerts anti-inflammatory effects against lipopolysaccharide by inducing autophagy. *Sci. Rep.* 10:3107.

Singh, S. B. & H. C. Lin. 2021. Role of intestinal alkaline phosphatase in innate immunity. *Biomol.* 11:1784.

Small, C. M., E. A. Beck, M. C. Currey, H. F. Tavalire, S. Bassham & W. A. Cresko. 2023. Host genomic variation shapes gut microbiome diversity in threespine stickleback fish. *mBio.* 14:e00219-00223.

Smith, J. L., G. Summers & R. Wong. 2010. Nutrient and heavy metal content of edible seaweeds in New Zealand. *New Zealand J Crop Horticult Sci.* 38:19–28.

Soo, R. M., C. T. Skennerton, Y. Sekiguchi, M. Imelfort, S. J. Paech, P. G. Dennis, J. A. Steen, D. H. Parks, G. W. Tyson & P. Hugenholtz. 2014. An expanded genomic representation of the phylum cyanobacteria. *Genome Biol. Evol.* 6:1031–1045.

Sparagon, W. J., E. C. Gentry, J. J. Minich, L. Vollbrecht, L. M. L. Laurens, E. E. Allen, N. A. Sims, P. C. Dorrestein, L. W. Kelly & C. E. Nelson. 2022. Fine scale transitions of the microbiota and metabolome along the gastrointestinal tract of herbivorous fishes. *Anim Microbiom.* 4:33.

Starr, A. E., S. A. Deeke, L. Li, X. Zhang, R. Daoud, J. Ryan, Z. Ning, K. Cheng, L. V. H. Nguyen, E. Abou-Samra, M. Lavallée-Adam & D. Figeys. 2018. Proteomic and metaproteomic approaches to understand host–microbe interactions. *Anal. Chem.* 90:86–109.

Stevenson, S. J. R., K. C. Lee, K. M. Handley, E. R. Angert, W. L. White & K. D. Clements. 2022. Substrate degradation pathways, conserved functions and community composition of the hindgut microbiota in the herbivorous marine fish *Kyphosus sydneyanus*. *Comp. Biochem. Physiol. A Mol. Integr. Physiol.* 272:111283.

Stone, D. A. J., J. O. Harris, H. Wang, G. J. Mercer, E. N. Schaefer & M. S. Bansemer. 2013. Dietary protein level and water temperature interactions for greenlip abalone *Haliotis laevigata*. *J Shellfish Res.* 32:119–130. 112.

Sunagawa, S., L. P. Coelho, S. Chaffron, J. R. Kultima, K. Labadie, G. Salazar, B. Djahanschiri, G. Zeller, D. R. Mende, A. Alberti, F. M. Cornejo-Castillo, P. I. Costea, C. Cruaud, F. d'Ovidio, S. Engelen, I. Ferrera, J. M. Gasol, L. Guidi, F. Hildebrand, F. Kokoszka, C. Lepoivre, G. Lima-Mendez, J. Poulain, B. T. Poulos, M. Royo-Llonch, H. Sarmento, S. Vieira-Silva, C. Dimier, M. Picheral, S. Searson, S. Kandels-Lewis, C. Bowler, C. de Vargas, G. Gorsky, N. Grimsley, P. Hingamp, D. Iudicone, O. Jaillon, F. Not, H. Ogata, S. Pesant, S. Speich, L. Stemmann, M. B. Sullivan, J. Weissenbach, P. Wincker, E. Karsenti, J. Raes, S. G. Acinas & P. Bork., Tara Oceans coordinators. 2015. Structure and function of the global ocean microbiome. *Science (1979).* 348:1261359.

Tahil, A. S. & M. A. Juinio-Menez. 1999. Natural diet, feeding periodicity and functional response to food density of the abalone, *Haliotis asinina* l., (gastropoda). *Aquacult Res.* 30:95–107.

Tanaka, R., I. Sugimura, T. Sawabe, M. Yoshimizu & Y. Ezura. 2003. Gut microflora of abalone *Haliotis discus hannai* in culture changes coincident with a change in diet. *Fish Sci.* 69:951–958.

Thomas, F., J.-H. Hehemann, E. Rebuffet, M. Czjzek & G. Michel. 2011. Environmental and gut bacteroidetes: the food connection. *Front. Microbiol.* 2:93.

Van Soest, P. 1994. Nutrional ecology of the ruminant. Ithica, NY: Cornell University Press.

Vileisis, A. 2020. Abalone: the remarkable history and uncertain future of California's iconic shellfish. Corvalis, OR: Oregon State University Press.

Villasante, A., N. Catalán, R. Rojas, K. B. Lohrmann & J. Romero. 2020. Microbiota of the digestive gland of red abalone (*Haliotis rufescens*) is affected by withering syndrome. *Microorganism.* 8: 1411

Walters, W., E. R. Hyde, D. Berg-Lyons, G. Ackermann, G. Humphrey, A. Parada, J. A. Gilbert, J. K. Jansson, J. G. Caporaso, J. A. Fuhrman, A. Apprill & R. Knight. 2016. Improved bacterial 16s rRNA gene (v4 and v4-5) and fungal internal transcribed spacer marker gene primers for microbial community surveys. *mSystems.* 1:e00009–00015.

Wang, W., M. J. Salini, H. Li, K. Mai & W. Zhang. 2024. Effect of dietary carbohydrate sources on growth performance and carbohydrate utilisation in abalone, *Haliotis discus hannai ino*. *Anim Feed Sci Technol.* 318:116143.

Whyte, J. N. C. & J. R. Englar. 1978. Seasonal changes in the content of non-metallic inorganic components in the marine alga *Macrocystis integrifolia*. Fisheries and Marine Service Technical Report 765. Vancouver, BC: Fisheries and Marine Service Department of Fisheries and the Environment, Canada. p. 33.

Wilson, J. M. & L. F. C. Castro. 2010. Morphological diversity of the gastrointestinal tract in fishes. In: M. Grosell, A. P. Farrell & C. J. Brauner, editors. The multifunctional gut of fish. San Diego: Elsevier. pp. 1–55.

Yao, Q., K. Yu, J. Liang, Y. Wang, B. Hu, X. Huang, B. Chen & Z. Qin. 2019. The composition, diversity and predictive metabolic profiles of bacteria associated with the gut digesta of five sea urchins in Luhuitou fringing reef (northern South China Sea). *Front. Microbiol.* 10:1168.

Yoshida, H., H. Sagami & S. Oikawa. 1977. Purification and properties of two acid phosphatases from midgut glands of abalone *Haliotis discus*. *J. Biochem.* 81:1447–1454.

Yu, W., Y. Lu, Y. Shen, J. Liu, S. Gong, F. Yu, Z. Huang, W. Zou, M. Zhou, X. Luo, W. You & C. Ke. 2022. Exploring the intestinal microbiota and metabolome profiles associated with feed efficiency in Pacific abalone (*Haliotis discus hannai*). *Front. Microbiol.* 13:852460.

Zeeman, Z., G. M. Branch, T. P. Peschak & D. Pillay. 2012. Assessing the ecosystem effects of the abalone *Haliotis midae* from its diet and foraging behaviour. *Afr J Mar Sci.* 34:205–214.

APPENDIX PHYLOGENETIC ANALYSES

Foot muscle tissue was acquired from abalone samples collected between 1996 and 2018 for seven species from the northeastern Pacific (*Haliotis corrugata, H. cracherodii, H. fulgens, H. kamtschatkana, H. rufescens, H. sorenseni,* and *Haliotis walallensis* (Stearns 1899) and one from New Zealand, *Haliotis iris* (Gmelin 1791) (Table A1). Tissue samples from the California taxa (except *H. fulgens*) were acquired from the University of California, Davis, Bodega Marine Laboratory. Epipodial clippings of *H. fulgens* were acquired from freshly harvested, live animals from Catalina Island, from Nancy Caruso of Get Inspired! Inc. Tissue from *H. iris* came from Te Papa Tongarewa Museum of New Zealand, after the animals were freshly collected in 2015 (Table A1). Before DNA extraction, tissues were stored in molecular-grade ethanol at 4°C.

The total DNA was extracted from the foot muscle using a DNeasy Blood and Tissue extraction kit (Qiagen, Valencia, CA) following the manufacturer's instructions. The tissue of 10–25 mg was blotted dry of ethanol and cut into small pieces before proceeding with the protocol. Extracted DNA was stored in the elution Buffer AE from the DNeasy protocol (10 mM Tris–Cl, 0.5 mM EDTA, pH 9.0) at 4°C until ready to be used for PCR reactions. Spectrophotometry (Synergy H1, BioTek, Winooski, VT) was used to quantify DNA concentration for each sample.

Following the methodology outlined by (Kim et al. 2014), PCRs were conducted to amplify sequences for two mitochondrial genes (16S rDNA and cytochrome *b*) and two nuclear genes (*h3* and a region spanning *its1* and *its2*). The concatenated sequence of all four gene regions was 2,171 bp with the following breakdown per gene; 545 bp of the 16S ribosomal DNA (16S) gene and 705 bp of the cytochrome *b* (cyt *b*) gene were obtained. The latter codes for a protein involved in transmembrane electron transfer in respiration (Degliesposti et al. 1993). A 342 bp region of the H3 (Histone 3) gene and a 579 bp portion of the internal transcribed spacer region 1, 5.8s rRNA, and internal transcribed spacer region 2 (hereafter ITS1-5.8S-ITS2) were obtained. Each PCR cycle consisted of an initial denaturation at 95°C for 2–3 min, followed by 35 cycles of: denaturation at 95°C for 30 sec, annealing (temperatures adjusted for each primer set) for 30–60 sec, extension at 72°C for 60–90 sec. The final extension step was at 72°C for 5 min. For 16S, an annealing temperature of 61°C was used (except for *Haliotis sorenseni, H. iris,* and *H. fulgens*, for which 59°C was used) with the following primers (Kim et al. 2014): 16SrDNAF 5′-CGC CTG TTT ATC AAA AAC AT-3′, 16SrDNAR 5′-CCG GTC TGA ACT CAG ATC ACG T-3′. For cyt *b*, an annealing temperature of 60°C was used with the following self-designed primers (Primer-BLAST, NCBI): cytbF3 5′-GTG CTC ACG TTG AGT TAG CTT-3′, cytbR2 5′-TAA ACA CAC GCC

TABLE A1.

Sampling dates and sources for the foot muscle tissues of each animal.

Species	Animal ID	Date collected	Source
Haliotis rufescens (*n* = 5)	SF07-3–1	February 5, 2007	Van Damme, CA
	SF07-25–133	July 18, 2007	Farallones Island, CA
	SF07-48–7	April 26, 2003	Soberanes Pt., CA
	SF10-15–1	May 14, 2010	Bodega Head, CA
	SF07-32–18	August 25, 2007	San Miguel Island, CA
Haliotis corrugata (*n* = 4)	SF08-6–3	2000	T. McCormick Broodstock
	SF02-24	pre1997	Hatchery Raised 1993, *Proteus*
	SF04-36–1	August 20, 2004	Cape Cortes, Santa Catalina Island
	SF08-6–2	2000	T. McCormick Broodstock
Haliotis walallensis (*n* = 2)	SF06-18–15	Nov 2003	Van Damme, CA
	SF08-48–1	unknown	Oregon
Haliotis kamtschatkana (*n* = 3)	SF15-52–2	August 17, 2015	Van Damme, CA
	SF15-52–3	August 17, 2015	Van Damme, CA
	SF15-52–4	August 17, 2015	Van Damme, CA
Haliotis cracherodii (*n* = 2)	SF03-34–2	1996	Ano Nuevo Island (S of San Francisco), CA
	SF03-31–30	pre2003	Carmel, CA
Haliotis sorenseni (*n* = 5)	SF08-25–2	2004	Santa Cruz Island (via Tom McCormick and BML)
	SF08-25–3	November 7, 2000	Farnsworth (via Tom McCormick and BML)
	SF03-20–1	November 8, 2000	Farnsworth (via CIMRI)
	SF08-25–1	March 28, 2000	Farnsworth (via Tom McCormick and BML)
	SF05-37–1	November 7, 2000	Farnsworth (via Tom McCormick)
Haliotis iris (*n* = 2)	M.318749 (6)	October 3, 2015	40° 39.82′ S, 172° 24.17′ E, New Zealand, South Island, Punapaua, W of Collingwood, M Young
	M.318749 (7)	October 3, 2015	40° 39.82′ S, 172° 24.17′ E, New Zealand, South Island, Punapaua, W of Collingwood, M Young
Haliotis fulgens (*n* = 2)	Cat-G01	January 13–14, 2018	Catalina Island
	Cat-G03	January 13–14, 2018	Catalina Island

The gene sequences from the one *Haliotis discus* individual included in the tree were from a full genome (Nam et al. 2017).

TABLE A2.

Isolate and GenBank accession numbers for each gene region of each individual (isolate) sequenced for phylogenetic analysis.

		Gene region			
Species	**Isolate**	**16S**	**cyt *b***	**H3**	**ITS1-5.8S-ITS2**
Haliotis rufescens	SF07-3–1	MH395949	MH427191	MH443024	MH443049
(*n* = 5)	SF07-25–133	MH395950	MH427192	MH443025	MH443050
	SF07-48–7	MH395951	MH427193	MH443026	MH443051
	SF10-15–1	MH395952	MH427194	MH443027	MH443052
	SF07-32–18	MH395953	MH427195	MH443028	MH443053
Haliotis corrugata	SF08-6–3	MH395945	MH427187	MH443020	MH443045
(*n* = 4)	SF02-24	MH395946	MH427188	MH443021	MH443046
	SF04-36–1	MH395947	MH427189	MH443022	MH443047
	SF08-6–2	MH395948	MH427190	MH443023	MH443048
Haliotis walallensis	SF06-18–15	MH395936	MH427180	MH443013	MH443038
(*n* = 2)	SF08-48–1	MH395937	MH427181	MH443014	MH443039
Haliotis	SF15-52–2	MH395942	MH427184	MH443017	MH443042
kamtschatkana	SF15-52–3	MH395943	MH427185	MH443018	MH443043
(*n* = 3)	SF15-52–4	MH395944	MH427186	MH443019	MH443044
Haliotis	SF03-34–2	MH395932	MH427176	MH443009	MH443034
cracherodii (*n* = 2)	SF03-31–30	MH395933	MH427177	MH443010	MH443035
Haliotis sorenseni	SF08-25–2	MH395955	MH427197	MH443030	MH443055
(*n* = 5)	SF08-25–3	MH395956	MH427198	MH443031	MH443056
	SF03-20–1	MH395957	MH427199	MH443032	MH443057
	SF08-25–1	MH395958	MH427200	MH443033	MH443058
	SF05-37–1	MH395954	MH427196	MH443029	MH443054
Haliotis iris (*n* = 2)	M.318749 (6)	MH395940	MH427182	MH443015	MH443040
	M.318749 (7)	MH395941	MH427183	MH443016	MH443041
Haliotis fulgens	Cat-G01	MH395934	MH427178	MH443011	MH443036
(*n* = 2)	Cat-G03	MH395935	MH427179	MH443012	MH443037

CAA TCC CT-3′. For *H. fulgens*, an annealing temperature of 57°C was used with a custom reverse primer that overlapped with cytbR2 but was more specific for *H. fulgens*: cytbR1 5′-GCC CAA TCC CTT CAA ATG GC-3′. Likewise, for *H. sorenseni*, primers designed to be specific to that species were used, and both overlapped with primers used the other taxa: cytbF1 5′-GGG GTT GTG TCT TGT TGT GC-3′ and cytbR3 5′-AGA ACA GTA AAC ACA CGC CCA-3′. For H3, a 60°C annealing temperature was used with the following designed primers: H3F 5′-ATG GCT CGT ACC AAG CAG AC-3′ and H3R 5′-TCC TTG GGC ATG ATG GTG AC-3′. For ITS1-5.8S-ITS2, the following primers (Coleman & Vacquier 2002) were used for all individuals unless specified, with an annealing temperature of 63°C: ABA-FOR 5′-TCG ATG AAG AGC GCA GCC-3′ and Hal-REV 5′-AGT CTC GTC TGA TCT GAG GTC-3′. Primers Hal-FOR 5′-TGA ACC TGC GGA AGG ATC ATT AAC G-3′, G-FOR 5′-GGG ATC CGT TTC CGT AGG TGA ACC TGC-3′, and G-REV 5′-GGG ATC CAT ATG CTT AAG TTC AGC GGG T-3′ were also used (Coleman & Vacquier 2002), with details on variations as follows: one *H. walallensis* sample was sequenced with primer sets Hal-FOR/Hal-REV and G-FOR/G-REV with an annealing temperature of 56°C. *H. cracherodii* was sequenced using primer set Hal-FOR/Hal-REV.

PCR products were visually inspected on 1% agarose gels, and then cleaned with a PCR NucleoSpin Gel and PCR Cleanup kit (Macherey-Nagel, Bethlehem, PA). Occasionally samples with faint extra bands were gel-extracted, both procedures following the manufacturer's protocol. Cleaned samples were sent to Eton Bioscience (San Diego, CA) for Sanger sequencing. Sequences from one *Haliotis discus* (Reeve, 1846) individual were extracted from the genome (Nam et al. 2017) using Blast 2.2.31. Sequences were aligned for each gene using CodonCode Aligner (v4.2.7) (CodonCode Corporation, Dedham, MA), and trimmed to the size of the shortest fragment. An open reading frame was determined for H3 using ORFfinder (NCBI), and the analysis was partitioned by codon for H3. All novel sequences were deposited on GenBank (NCBI, accession numbers in Supplemental Table S2).

Phylogenetic relationships were generated using a mixed-model, partitioned Bayesian method as implemented in the software package Mr. Bayes version 3.2.6 (Ronquist et al. 2012). Analyses were conducted on concatenated sequences of all genes, partitioned by gene, as well as separate analyses for each nuclear or mitochondrial marker. Ten million generations of Markov Chain Monte Carlo sampling were performed using a random starting topology with trees sampled every 200 generations, with 25,000 early runs counted as burnin. The retained 50,002 trees were used to construct a 50% majority rule consensus tree. The percentage of times that a particular node was recovered in the analysis is interpreted as the posterior probability of the occurrence of that node. Phylogenetic trees were created using FigTree (v1.4.2) and rooted with *H. iris* (New Zealand) because all gene-trees or phylogenies to date show *H. iris* as an outgroup to a clade containing northeastern Pacific taxa (Lee & Vacquier 1992, Coleman & Vacquier 2002, Estes et al. 2005, Geiger & Owen 2012).

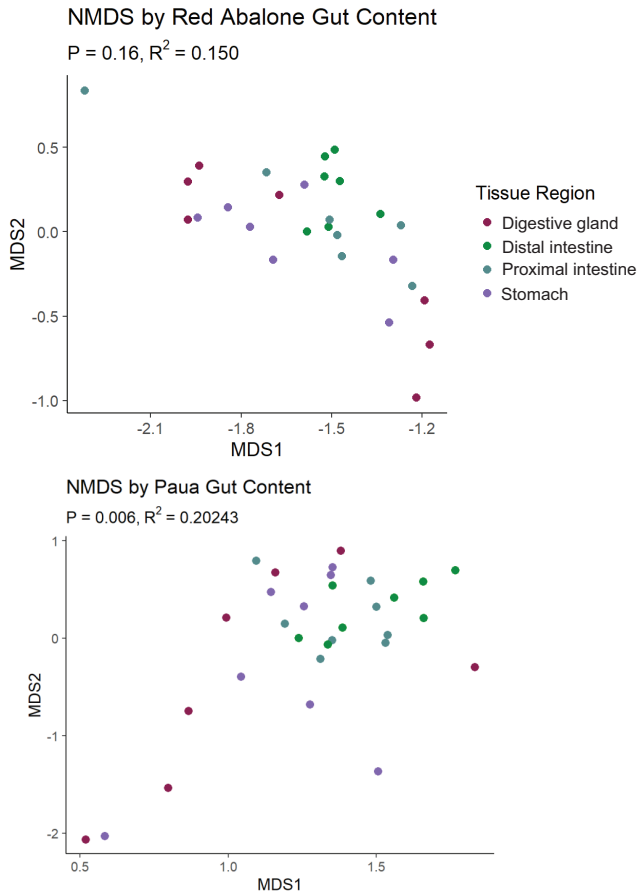

Figure A1. Nonmetric multidimensional scaling plot based on Bray–Curtis Dissimilarity of the microbial communities in the contents of various gut regions of the abalone species *Haliotis rufescens* (red abalone) and *Haliotis iris* (pāua). Proximity to other symbols indicates similarity.

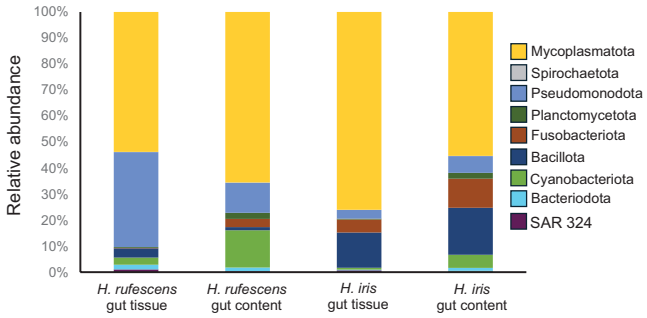

Figure A2. Stacked bar plot of relative frequency of microbial communities (at the phylum level) in the gut tissues and gut contents of the abalone species *Haliotis rufescens* and *Haliotis iris*. The key on the side depicts the phyla. These phyla are also represented but are too small to see (each representing <0.03%): Actinobacteriota, Campilobacterota, Chloroflexota, Desulfobacterota, Myxococcota, Verrucomicrobiota.